Two Boat Lake catchment

Field guide for a safety assessment analyst

Tobias Lindborg[1], Emma Johansson[1], Johan Rydberg[2], Peter Saetre[1], Lillemor Claesson Liljedahl[1]

1 Swedish Nuclear Fuel and Waste Management Co.
2 Department of Ecology and Environmental Science, Umeå University

2018

This field guide

In your hand you hold a field guide to the Two Boat Lake catchment (TBL). It is to be used as a supporting document when visiting the TBL-site and the surrounding Kangerlussuaq area in West Greenland when traveling together with the authors of this guide. The guide, with its illustrations has been put together by using a long list of already published work, or work in progress related to the GRASP project led and financed by Swedish Nuclear Fuel and Waste Management Company (SKB). The GRASP project is a joint activity between SKB, Stockholm University and Swedish University of Agricultural Sciences (SLU). Also other scientific institutions and research companies have been involved in the project and the reader is referred to individual articles or reports for a total co-author affiliation list. The overarching aim with the project is to enhance the understanding of biosphere properties and processes in periglacial environments and to be able to conceptually and numerically describe tundra type catchment elemental transport behaviour; an understanding not only of the present, but also into the far future linked with possible associated climate changes. To link these biosphere studies with the geosphere, a final section provides an overview of the Greenland Analogue Project (GAP), and shows some illustrations related to deep bedrock drilling and ice sheet investigations made in the Kangerlussuaq area (Claesson Liljedahl et al. 2016, Harper et al. 2016).

The guide illustrates selected parts of the work done and the result gained at the TBL-site during the period 2010 to 2017 and is intended to be used for illustrative purposes in the field only. Methods and assumptions made as well as resulting synthesis are not further discussed in this field guide and the reader is referred to the published articles and reports that constitute the scientific basis for the data presented in this guide (see list of references below).

After having clearly stated the above, enjoy the illustrations and please do not forget to bring a copy of this guide with you when entering the landscapes of the West Greenland tundra with its permafrost and pro- and periglacial processes.

References used

- Aaltonen I, Douglas B, Claesson Liljendahl L, Frape S, Henkemans E, Hobbs M, Klint K E, Lehtinen A, Lintinen P, Ruskeeniemi T, 2010. The Greenland Analogue Project, Sub-Project C, 2008, Field and data report. Posiva Working Report 2010-62, Posiva Oy, Finland.
- Claesson Liljedahl, L., Kontula, A., Harper, J., Näslund, J-O., Selroos, J-O., Pitkänen, P., Puigdomenech, I., Hobbs, M., Follin, S., Hirschorn, S., Jansson, P., Kennell, L., Marcos, N., Ruskeeniemi, T., Tullborg, E-L. & Vidstrand, P. (2016). The Greenland Analogue Project: Final report. (SKB report series TR-14-13). Svensk Kärnbränslehantering AB. Stockholm, Sweden.
- Eichinger F, Waber H N, 2013. Matrix porewater in crystalline rocks: extraction and analysis. NWMO TR-2013-23, Nuclear Waste Management Organization, Canada.
- Engström J, Klint K E S, 2014. Continental collision structures and post-orogenic geological history of the Kangerlussuaq area in the southern part of the Nagssugtoqidian orogen, Central West Greenland. Geosciences 4, 316–334.
- Follin S, Johansson P-O, Hartley L, Jackson P, Roberts D, Marsic N, 2007. Hydrogeological conceptual model development and numerical modelling using CONNECTFLOW, Forsmark modelling stage 2.2. SKB R-07-49, Svensk Kärnbränslehantering AB.
- Garde A A, Hollis J A, 2010. A buried Paleoproterozoic spreading ridge in the northern Nagssugtoqidian orogen, West Greenland. In Kusky T M, Zhai M-G, Xiao W (eds). The evolving continents : understanding processes of continental growth. London: Geological Society. (Special publications 338), 213–234.
- Garde A A, Marker M, 2010. Geological map of Greenland, 1:500 000, Kangerlussuaq/Søndre Strømfjord – Nuussuaq, Sheet 3. 2nd ed. Copenhagen: Geological Survey of Denmark and Greenland.
- Graly J A, Humphrey N F, Landowski C M, Harper J T, 2014. Chemical weathering under the Greenland Ice Sheet. Geology 42, 551–554.
- Harper J, Hubbard A, Ruskeeniemi T, Claesson Liljedahl L, Kontula A, Brown J, Dirkson A, Dow C, Doyle S, Drake H, Engström J, Fitzpatrick A, Follin S, Frape S, Graly J, Hansson K, Harrington J, Henkemans E, Hirschorn S, Hobbs M, Humphrey N, Jansson P, Johnson J, Jones G, Kinnbom P, Kennell L, Klint K E S, Liimatainen J, Lindbäck K, Meierbachtol T, Pere T, Pettersson R, Tullborg E-L, van As D, 2016a. The Greenland Analogue Project: Data and Processes. SKB R-14-13, Svensk Kärnbränslehantering AB.

- Harper J, Hubbard A, Ruskeeniemi T, Claesson Liljedahl L, Lehtinen A, Booth A, Brinkerhoff D, Drake H, Dow C, Doyle S, Engström J, Fitzpatrick A, Frape S, Henkemans E, Humphrey N, Johnson J, Jones G, Joughin I, Klint K E, Kukkonen I, Kulessa B, Landowski C, Lindbäck K, Makahnouk M, Meierbachtol T, Pere T, Pedersen K, Pettersson R, Pimentel S, Quincey D, Tullborg E-L, van As D, 2011. The Greenland Analogue Project. Yearly report 2010. SKB R-11-23, Svensk Kärnbränslehantering AB.
- Johansson, E. (2016). The influence of climate and permafrost on catchment hydrology. ISSN: 1653-7211. Department of Physical Geography, Stockholm University
- Johansson, E., Berglund, S., Lindborg, T., Petrone, J., van As, D., Gustafsson, L-G., Näslund, J-O. & Laudon, H. (2015a). Hydrological and meteorological investigations in a periglacial lake catchment near Kangerlussuaq, west Greenland – presentation of a new multi-parameter data set. *Earth System Science Data*, vol. 7, pp. 93–108, doi:10.5194/essd-7-93-2015.
- Johansson, E., Gustafsson, L-G., Berglund, S., Lindborg, T., Selroos, J-O., Claesson Liljedahl, L. & Destouni, G. (2015b). Data evaluation and numerical modeling of hydrological interactions between active layer, lake and talik in a permafrost catchment, Western Greenland. *Journal of Hydrology*, vol. 527, pp. 688–703.
- Lindborg, T., 2017. Climate-driven Landscape Development: Physical and Biogeochemical Long-term Processes in Temperate and Periglacial Environments. Doctoral thesis. Swedish University of Agricultural Sciences978-91-7760-039-8.
- Lindborg, T., Rydberg, J., Andersson, E., Löfgren, A., Johansson, E., Saetre, P., Sohlenius, G., Berglund, S., Kautsky, U. & Laudon, H. (submitted). Terrestrial and Aquatic Pools and Fluxes in a Periglacial Landscape: Carbon Budget Analysis for a Catchment in West Greenland.
- Lindborg, T., Rydberg, J., Lidman, F., Tröjbom, M., Berglund, S., Johansson, E., Kautsky, U. & Laudon, H. (manuscript). Mass-balance of 42 elements in a periglacial lake catchment in West Greenland.
- Lindborg, T., Rydberg, J., Tröjbom, M., Berglund, S., Johansson, E., Löfgren, A., Saetre, P., Nordén, S., Sohlenius, G., Andersson, E., Petrone, J., Borgiel, M., Kautsky, U. & Laudon, H. (2016). Biogeochemical data from terrestrial and aquatic ecosystems in a periglacial catchment, West Greenland. *Earth System Science Data*, vol. 8, pp. 439-459.
- Pere T, 2014. Geological logging of the Greenland Analogue Project drill cores DH-GAP01, 03 and 04. Posiva Working Report 2013-59, Posiva Oy, Finland.
- Petrone, J., Sohlenius, G., Johansson, E., Lindborg, T., Näslund, J-O., Strömgren, M., & Brydsten, L. (2016). Using ground-penetrating radar, topography and classification of vegetation to model the sediment and active layer thickness in a periglacial lake catchment, western Greenland. *Earth System Science Data*, vol. 8, pp. 663-677.
- Rydberg, J., Lindborg, T., Solenius, G., Reuss, N., Olsen, J. & Laudon, H. (2016). The importance of eolian input on lake sediment geochemical composition in the dry proglacial landscape of western Greenland. *Arctic, Antarctic and Alpine Research*, vol. 48, pp. 93– 109.
- Sjöberg, Y., E. Coon, A. B. K. Sannel, R. Pannetier, D. Harp, A. Frampton, S. L. Painter, and S. W. Lyon., 2016, Thermal effects of groundwater flow through subarctic fens: A case study based on field observations and numerical modeling, Water Resour. Res., 52, 1591–1606, doi:10.1002/2015WR017571
- Sjöberg, Y., Johansson, E., Rydberg, J. (2017) Flow Pathways of Snow and Ground Ice Melt Water During Initial Seasonal Thawing of the Active Layer on Continuous Permafrost, American Geophysical Union Fall Meeting 2017, 2017-12-13, New Orleans, USA.
- Tedesco M, Fettweis X, Alexander P, Green G, Datta T, 2013. MAR Greenland Outputs 1958–2013 ver. 3.2, CCNY Digital Archive. https://www.aoncadis.org/dataset/CPL_MAR.html.
- van As, D., Fausto, R. S., and PROMICE Project Team. Programme for Monitoring of the Greenland Ice Sheet (PROMICE): first temperature and ablation records. Geol. Surv. Denmark Greenland Bull., 23, 73-76. 2011.
- van As, D., Hubbard, A. L., Hasholt, B., Mikkelsen, A.B., Van den Broeke, M.R., and Fausto R.S.: Large surface meltwater discharge from the Kangerlussuaq sector of the Greenland ice sheet during the record-warm year 2010 explained by detailed energy budget observations. Cryosph., 6, 199-209 (doi: 10.5194/tc-6-199-2012), 2012.
- van Tatenhove, F.G.M., van der Meer, J.J.M. & Koster, E.A. (1996). Implications for deglaciation chronology from new AMS age determinations in central west Greenland. *Quaternary Research*, vol. 45, pp. 245–253.

Table of content

West Greenland and the Kangerlussuaq area

Kangerlussuaq settlement

The settlement is divided into three distinct areas: the airport, the airbase and the old part (Fig. 1). Apart from the roads around and within the settlement of Kangerlussuaq there is only one road that extends out from the settlement. This road goes from the harbour south west of Kangerlussuaq to the ice sheet in north east and is approximately 50 km long (Fig. 2).

Figure 1. *Top: Kangerlussuaq settlement map. Background photo taken from google maps. Bottom: Kangerlussuaq photograph heading west. Photo by Tobias Lindborg.*

Kangerlussuaq area

The Kangerlussuaq region is the part of southwestern Greenland where the distance from the coast to the ice sheet is the largest, approximately 200 km. The position far from the sea and the proximity to the ice margin influences the local climate (Claesson Liljedahl et al. 2016). There are a large number of proglacial lakes in the ice-free part of the area (Fig. 2).

The Kangerlussuaq village has a population of approximately 500 people and is centred on the Kangerlussuaq International Airport (SFJ), which is the largest civilian airport in Greenland. In Greenlandic terms it is an easily accessible area, which in combination with the access to the Kangerlussuaq International Science Support centre (KISS) and the gravel road leading up to the ice sheet and Point 660, forming an easy access point to the ice sheet makes the area an international research hub (Claesson Liljedahl et al. 2016).

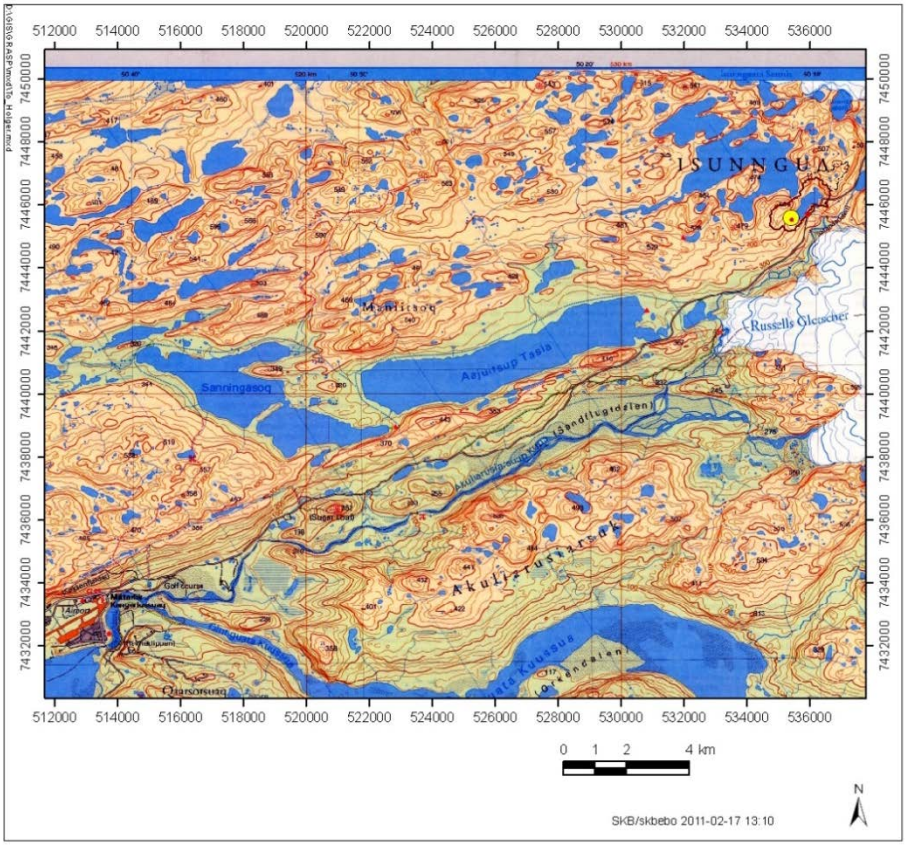

Figure 2. *Map of Kangerlussuaq area with the road to the ice sheet. Two Boat lake catchment encircled in red at upper right corner. Kangerlussuaq settlement located in lower left corner. Yellow dot = Drill hole GAP01.*

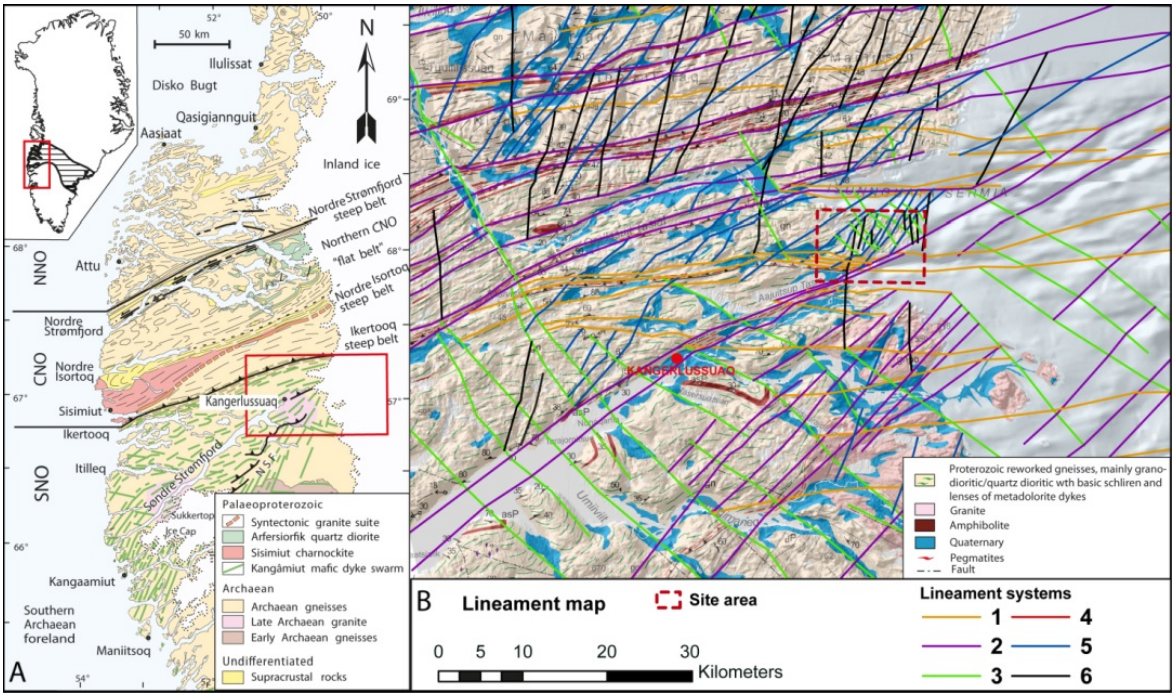

Figure 3. *A) Geological map of the central western Greenland and the Nagssugtoqidian orogeny. B) Lineament and geologic map of the GAP study area, where the red dashed rectangle denotes the area where the GAP carried out geologic mapping. (Map modified from Garde and Marker 2010, and Garde and Hollis 2010).*

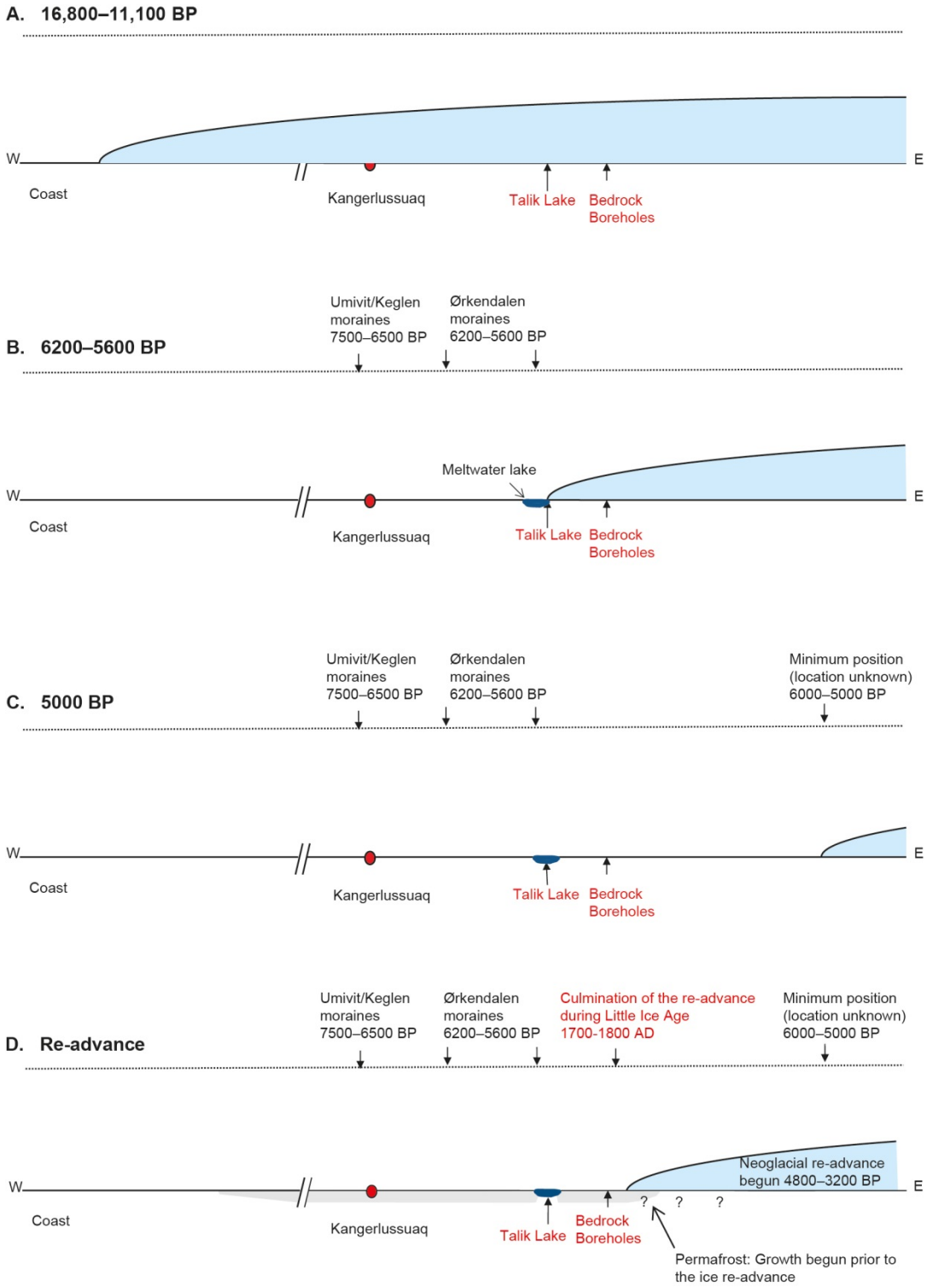

Figure 4. *Cartoon showing the deglaciation history of the Kangerlussuaq area since the Last Glacial Maximum (LGM). Many of the present lakes were likely formed as soon as the area was exposed from the retreating ice sheet. These lakes were first filled with meltwaters and later turned into non-glacial lakes, implying that the growth of permafrost was prevented under these lakes when the climate started to cool during the neoglacial re-advance. Moraine ages are presented as* ^{14}*C BP and are from van Tatenhove et al. (1996). Talik lake corresponds to Two Boat Lake catchment.*

The GRASP project

The aim of the Greenland Analogue Surface Project (GRASP) is two-fold. The first part is focused on how ecosystems develop and react in a long-term climate change perspective during an entire glacial cycle (Lindborg 2017). The other part aimed at improving the understanding of water exchanges between surface water and groundwater in a periglacial environment. Hydrological and biogeochemical processes and conditions not considered in temperate climate regions may be of great importance in periglacial areas. Hydrological responses in these cold areas differ in fundamental aspects from catchments in boreal and temperate regions. Most importantly, the hydrology in periglacial environments is intimately connected to the presence of permafrost and the active layer dynamics. Snow related processes have also been shown to be of great importance for the annual water balance. These special hydrological conditions have in turn great impact on biogeochemical processes since the hydrology, together with eolian transport, are the main drivers for transport of elements in the landscape.

The aim of the hydrological field studies illustrated here was to identify and quantify the main hydrological processes in a periglacial lake catchment, thereby providing input to conceptual and mathematical modelling. The overarching target when planning the hydrological TBL field programme was to identify and quantify the main hydrological processes including the interactions between surface water in the lake and in the surrounding catchment, and the role of both supra- and sub-permafrost groundwater. Besides the scientific questions to be answered, the hydrological measurement program was to large extent determined by what was possible, given the hydrologic, climatic and logistic conditions at the site. Due to its remote location, but also depending on the harsh climate, the site has been manned only during relatively short periods. This limited the possibilities for long-term or continuous observations of some parameters that could not be measured automatically (e.g. surface water inflow to the lake or groundwater monitoring in the active layer). Lack of infrastructure for electrical power and telecommunications has also been a limiting factor. Typically three field campaigns per year (in April, June and August-September) have been organized during the period for which data are presented.

The general biogeochemical sampling and investigation strategy was to get a broad picture of element distribution and not to focus on any specific target element. The aim was to provide understanding of the general fluxes of dissolved and particulate matter in the system. Sample analyses were made for concentrations of carbon, nitrogen and phosphorus, together with associated species and isotopic composition, as well as total concentrations of a long list of major and trace elements and isotopes, which together with the hydrological model helped us to understand and calculate fluxes in the landscape. Age determinations of soils and sediment layers, together with estimates of biomass and primary production in both the terrestrial and aquatic systems, made it possible to calculate accumulation of various elements in different landscape and ecosystem units.

Two Boat Lake catchment (TBL)

Since 2010, the GRASP-project has collected hydrological and biogeochemical data in the TBL catchment (Fig. 5) with the aim to better understand periglacial landscapes (Johansson et al. 2015a, 2015b; Lindborg et al. 2016). In addition to constraining the geometry of the catchment (e.g., soil volumes and bathymetry; Table 1), Petrone et al. (2016) determined that the quaternary deposits consist mainly of till and glaciofluvial deposits that are overlain by an – on average – 1-m thick layer of eolian silt.

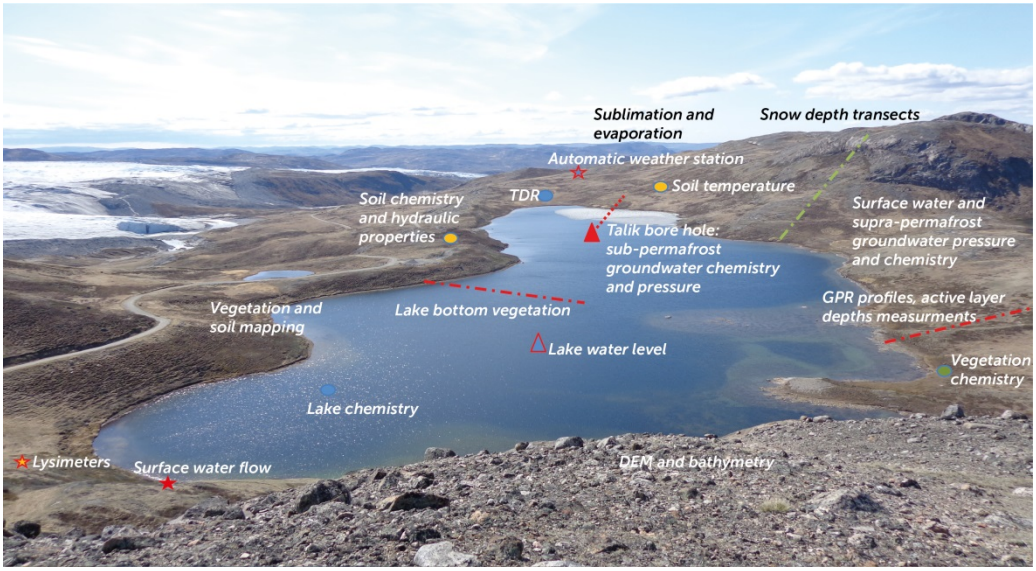

Figure 5. *Photo of TBL catchment with a general description of the location of sampling and monitoring points*

Johansson et al. (2015a; 20015b) studied the hydrology of the TBL-catchment, and report that the long term mean annual precipitation is 269 mm of which 40% falls as snow and that the potential evapotranspiration is 400 mm. They also conclude that there are no permanent streams, but that small intermittent streams appear during the snow-melt period, and that lake water outflow occurs only occasionally.

Table 1. Two Boat Lake system parameters describing catchment geometry and hydrology (from Lindborg 2017).

Terrestrial system parameter or pool	**Value**	**Reference or comment**
Precipitation, m^3yr^{-1}	348,000	Johansson et al. (2015a)
Evapotranspiration, m^3yr^{-1}	257,500	Johansson et al. (2015a)
Runoff to lake (excl. trans. area), m^3yr^{-1}	90,600	Johansson et al. (2015a)
Runoff related to snowmelt, m^3yr^{-1}	39,000	Johansson et al. (2015a)
Runoff transient area, m^3yr^{-1}	29,600	Johansson et al. (2015a)
Groundwater active layer, m^3	343,625	Johansson et al. (2015b)
Terrestrial catchment area, km^2	1.19	Petrone et al. (2016)
Terrest. catchm. incl. transient, km^2	1.70	Petrone et al. (2016)
Active layer depth, m	0.5	Petrone et al. (2016)
Permafrost soil depth (thickn. of silt), m	1	Petrone et al. (2016)
Active layer catchment volume, m^3	553,350	93% of terrest. catchm., 0–0.5 m
Permafrost soil volume, m^3	553,350	93% of terrest. Catchm., 0.5–1 m
Limnic system parameter or pool		
Precipitation, m^3yr^{-1}	100,100	Johansson et al. (2015a)
Evaporation, m^3yr^{-1}	179,100	Johansson et al. (2015a)
Lake water outflow, m^3yr^{-1}	5,300	Johansson et al. (2015a)
Groundwater recharge to talik, m^3yr^{-1}	6,300	Johansson et al. (2015a)
Lake water residence time, years	47	Lake volume/runoff to lake
Lake water solutes residence time, years	370	Lake volume/ (outflow + recharge)
Lake area, km^2	0.37	Johansson et al. (2015b)
Lake volume, m^3	4,290,000	Johansson et al. (2015b)
Lake maximum depth, m	29.9	Lindborg et al. (2016a)
Lake mean depth, m	11.3	Lindborg et al. (2016a)

In table 1 the catchment geometry and hydrological parameters for TBL are listed. This data are the synthesized result of both direct measurements and modelling exercises. For methods and further details we refer to the references listed in the table.

TBL installations and monitoring equipment

Weather station

The weather station (AWS), was installed on April 13, 2011 and is situated about 70 m from the lake (Fig. 6). The station is similar to approximately 20 other AWS installed on the ice sheet within the framework of the Programme for Monitoring of the Greenland Ice Sheet (PROMICE) (van As et al., 2011), of which three are located in the Kangerlussuaq region (van As et al., 2012). The station at TBL measures air temperature (~2.55 m above ground), air pressure, humidity (~2.55 m above ground), wind speed and direction (~3.05 m above ground), and the downward and upward components of shortwave (solar) and longwave (terrestrial) radiation (Table 2). A sonic ranger was mounted on the AWS to register changes in surface level due to the presence of snow. An important addition to the station, compared to the PROMICE stations located on the ice sheet, is a precipitation gauge capturing both snow and rain. The snow is melted in the gauge and the Snow Water Equivalent (SWE) is measured. All variables are recorded every ten minutes and processed to provide hourly averages. Data is stored locally, and averages (hourly and daily, for summer and winter, respectively) are transmitted via satellite. Details about the instrumentation (and online weather data) are given on http://www.promice.org.

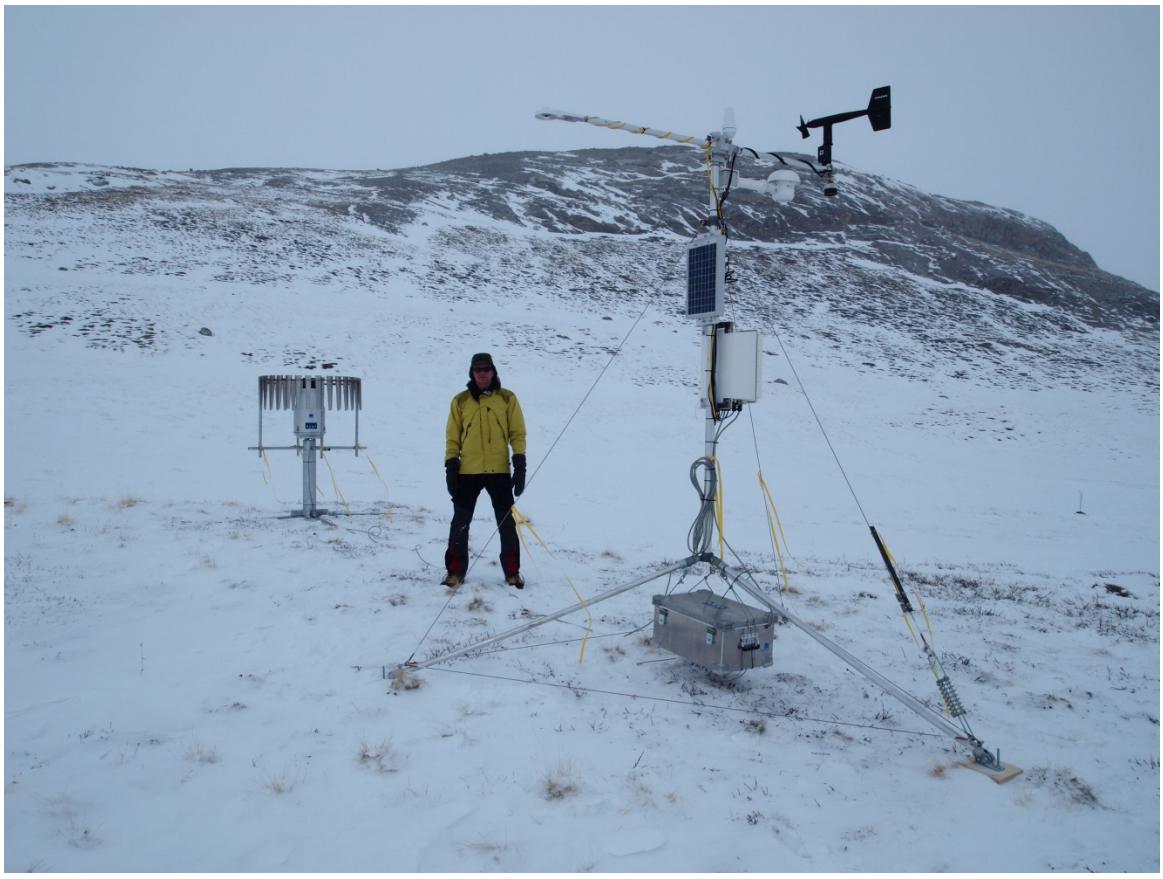

Figure 6. *Sten Berglund at the automated weather station during installation in April 2011. Photo: Tobias Lindborg.*

Table 2. List of used equipment, start of monitoring and time resolution and accuracy for each parameter for all monitoring data.

Parameter	Equipment	Monitoring started	Time resolution	Accuracy
Precipitation	Geonor T-200B	April 2011	10 min	
Air humidity, Barmometric pressure, Wind speed, Wind direction, Long and short wave radiation, Air temperature	See http://www.promice.org	April 2011	See http://www.promice.org	See http://www.promice.org

Not surprisingly, the weather data shows a pronounced annual cycle in air temperature at the study site (Fig. 7). Highest measured daily average temperature on record is 13°C and occurred in July 2016. Above freezing temperatures also occur several times each winter, implying that there is more than one snow melt event per year. Winter temperatures are often in the range from -10 to -20°C, although hourly measurements occasionally are below -30°C.

Wind speeds are typically low, with values below 5 m/s. Events with wind speeds exceeding 10 m/s occurs mostly in winter. During summer, the wind direction is almost exclusively from northeast to southeast, i.e., blowing down from the ice sheet. In winter, when storms are more frequent, the situation is reversed and westerly winds are more common. Irrespective of the season, the strongest winds originate from the southeast, in which direction the distance to the ice sheet is only one kilometre.

The mean annual corrected precipitation for the period 2012 - 2016 is 279 mm (Table 3). This is about 120 mm higher than the long-term mean-annual precipitation measured in Kangerlussuaq for the period 1977-2013. This indicates a gradient with increasing precipitation from the Kangerlussuaq settlement to the ice sheet. Most precipitation falls in April-May and August-October, and approximately 40% of the annual precipitation fall as snow.

Table 3. Annual precipitation (mm) for the period 2011 to 2017.

Year	P (mm)
2011	107*
2012	365
2013	269
2014	238
2015	280
2016	241
2017	283**
*from april	**until August

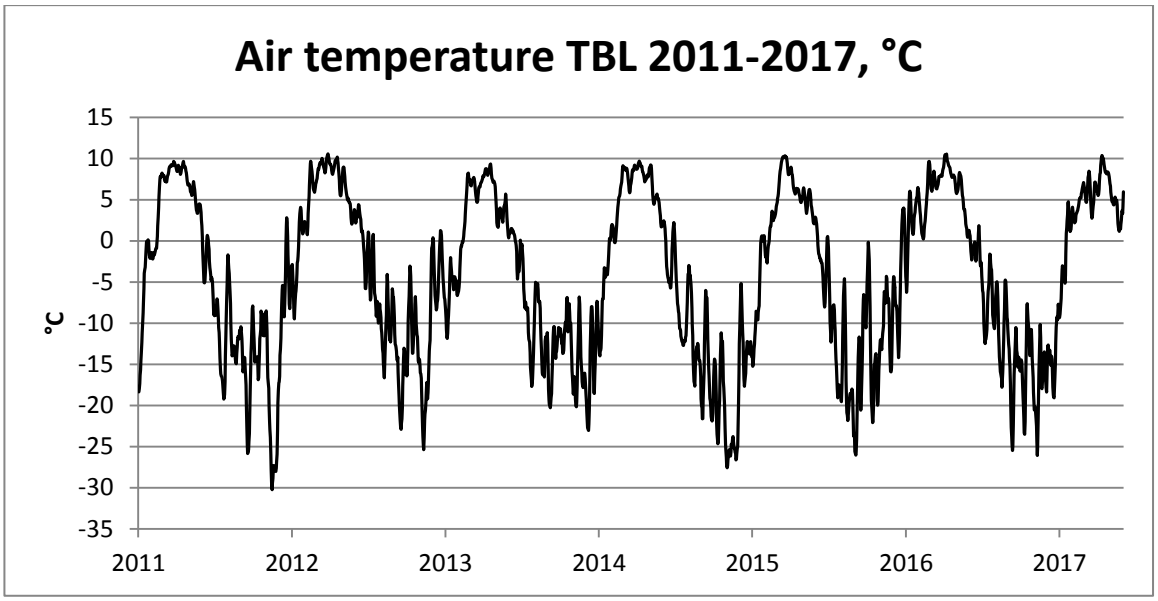

Figure 7. *Air temperature at TBL (KAN_B) from April 2011 to August 2017.*

Lake and groundwater level

Surface water levels are monitored using pressure transducers (Fig. 8 and 9) placed at the lake bottom both in TBL and in the lake located north-west of TBL (Fig. 2). The north-western lake, which is located at an elevation approximately 19 m above the TBL water level, is monitored with the purpose to get a reference lake level fluctuation in the area. This is also a precipitation driven lake but belongs to a different surface water system and discharges into a lake situated south of TBL. The transducers were placed at a minimum depth of 5 m to avoid disturbance from ice during the winter. Total pressure (hydrostatic and barometric) and temperature were logged every third hour. Data for the period 2010 to 2017 is shown in Fig. 10.

Figure 8. *Installation of the pressure transducer measuring the water level fluctuation in TBL.*

The variation in the lake-water level in TBL over the monitoring period is approximately 40 cm (Fig. 10). Generally the lake level increases during snow melt and drops in summer, however there are also clear inter-annual variability. The very dry summer of 2011 resulted in the lowest lake level on record, while the wet 2012 caused a considerable increase in the lake level. During the measurement period the lake level never reach the threshold of the lake, which is at approximately 20 cm above the reference level at start of measurements in September 2010. However, in spring 2014 and 2015 the lake level almost reached the threshold causing an outflow. The annual variation in the north-western Lake during the period 2012-2016 was 25 cm and there is a clear co-variation between the levels in the two lakes.

Figure 9. *Pressure transducer measuring the water level fluctuation in TBL.*

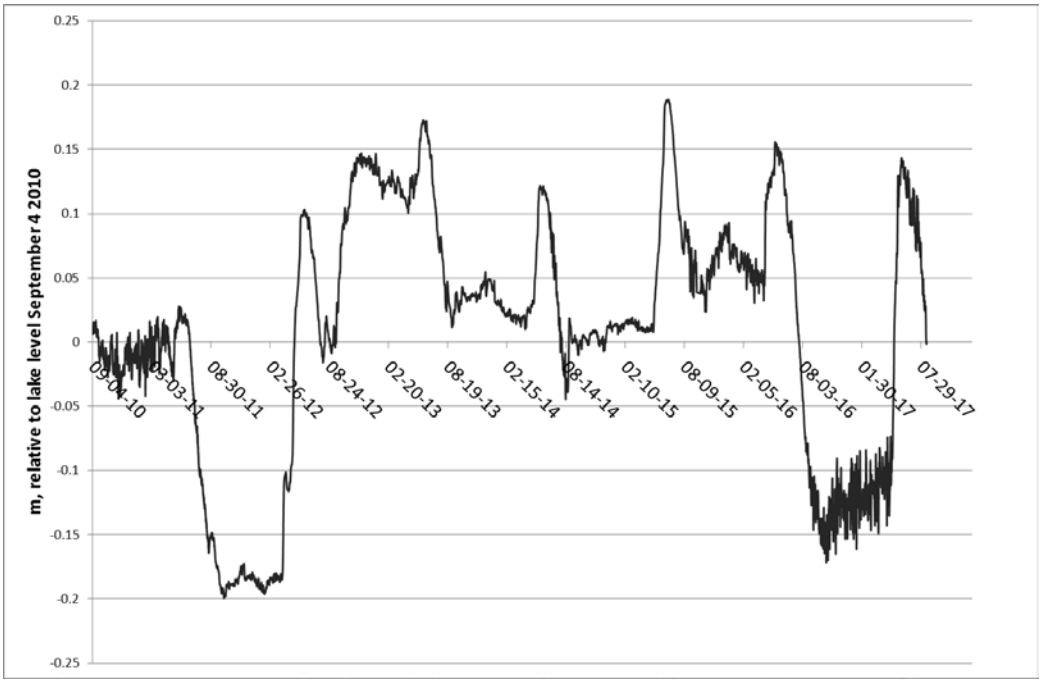

Figure 10. *Lake water level in TBL for the period Sept 2010 – Sept 2017.*

Soil temperature

A soil temperature station consisting of seven subsurface temperature sensors reaching a total depth of 2 m (with an additional sensor measuring air temperature at 1.6 m above ground) was installed in September 2010 (Fig. 11). Installation was done by drilling a hole with a diameter of approximately 60 mm through the active layer into the permafrost. In order to make sure that the sensors were placed at the right depths, the cables and sensors were attached to a PVC pipe, which was placed in the borehole. The sensors were connected to data loggers that were installed in boxes placed on the ground surface; the boxes and cables were covered by a mound of stones in order to protect them from animals, ice and snow.

Six additional soil temperature stations have been installed during the period 2012 to 2016. Those stations are shallow, reaching a depth of approximately 0.4 m. The main purpose with these stations is to analyse soil temperature and together with soil moisture. The shallow stations are situated close to the TDR-stations in the north-east and south western valleys of the catchment. One soil moisture station has also been installed at the lake threshold with the aim analyse weather there is a seepage of lake water across the water divide in the subsurface system.

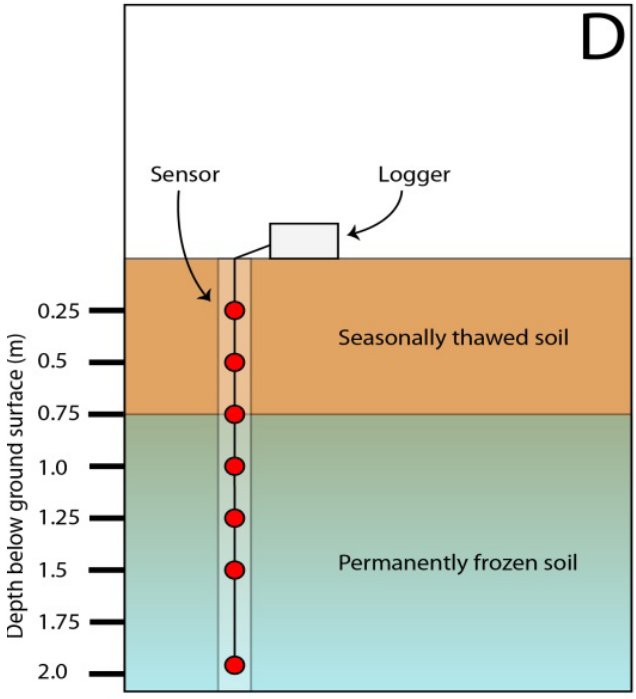

Figure 11. *Schematic figure over the soil temperature stations at TBL. One station has 7 sensors equally distributed to 2 m depth and the other six stations have 4 sensors evenly distributed over the depth of the active layer.*

At the deep soil temperature station, the transition from permafrost to the active layer occurs at approximately 0.9 m in late summer when the active layer is thickest (Fig. 12). The temperature sensor at 0.75 m depth have recorded temperatures above 0°C at least on one occasion every year since the monitoring started, whereas the sensor at 1 m depth has been continuously frozen with a maximum temperature of -0.1°C. The variations between the monitored years were relatively small. The thaw at 0.25 m depth, i.e., in the active layer, started in late May or early June and the freezing at that depth occurred in late September or early October. The maximum recorded temperature at 0.25 m depth occurred in July 2017. There is a decreasing co-variation between air and soil temperatures with depth resulting in a delay of freezing and thawing at larger depth, i.e. the active layer both thawed and froze from above.

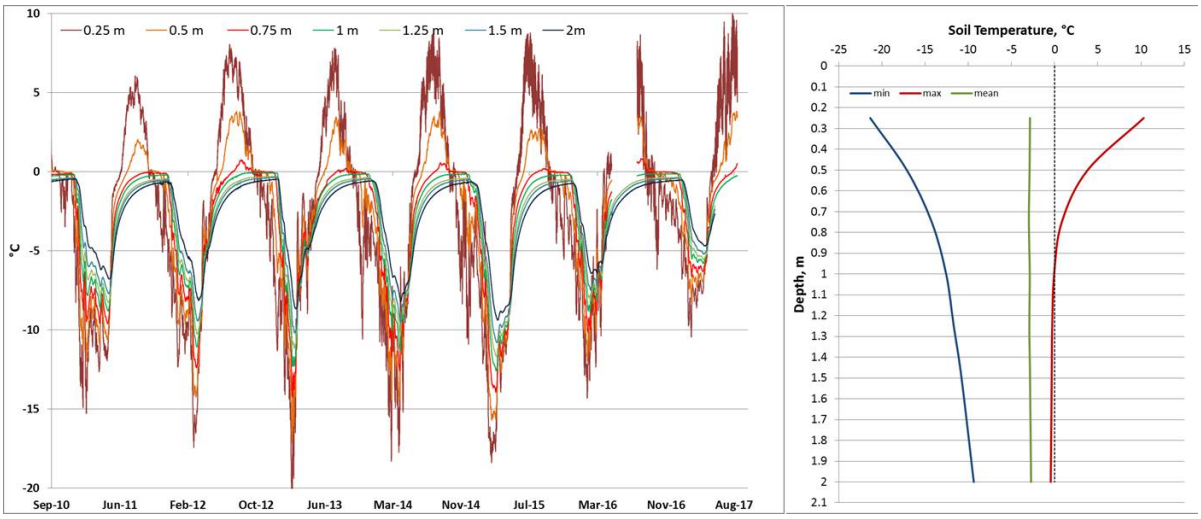

Figure 12. *Soil temperature data for the period 2010-2017 (left figure). In the right figure the minimum, maximum and mean temperatures for each depth are plotted.*

Soil water content measured in TDR transects

Spatial and temporal variations of soil water content are monitored by use of the Time Domain Reflectometry technique (TDR). In September 2011, 43 TDR-sensors were installed in three clusters within the catchment (Fig. 13). Each cluster consists of a number of depth profiles where TDR sensors are placed so that they cover the whole interval from just below the ground surface to the permafrost surface that constituted the bottom of the active layer at the time of installation. Clusters 1 and 2 consist of four depth profiles where the four sensors in each profile were distributed evenly from a depth of 5-10 cm below ground to a depth of 40-50 cm (Fig. 13A). The sensors in Cluster 3 are arranged in three depth profiles, each profile containing four sensors, which were placed along a transect from the lake into the catchment (Fig. 13C). The different clusters were arranged so that they form transects both along and transverse to the dominating flow direction, which generally was judged to be perpendicular to the lake shoreline.

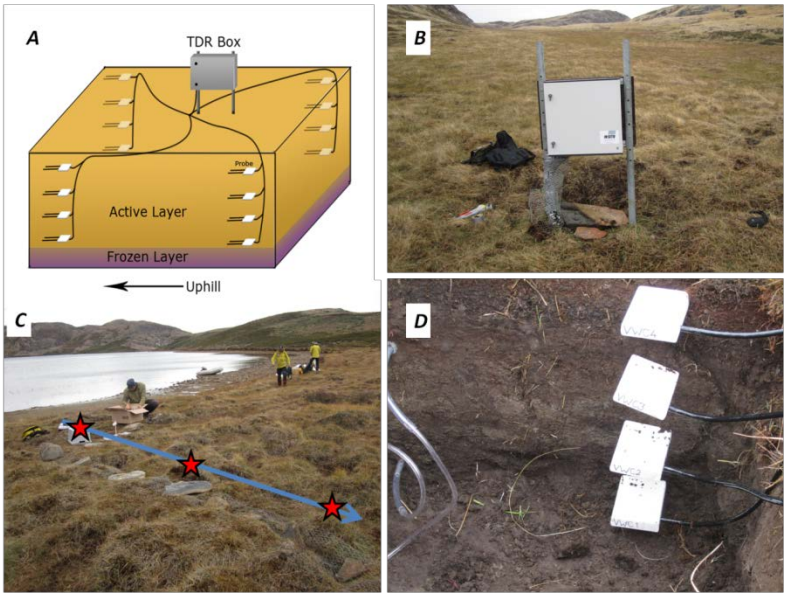

Figure 13. *TDR and lysimeter installation at TBL catchment. In figure A, a schematic figure of the logger (B), the depth profiles (C) and sensors installed in the active layer (D) is shown.*

Time series data on soil water content, given as volume of water per total volume of soil, is available from late August 2011. Figure 14 shows examples of soil water contents at different depths as functions of time and precipitation during the period from May to November 2014. The quick changes in apparent soil water content during autumn and late spring are due to a phase change from water to ice or from ice to water in the soil matrix. The figure illustrates how the active layer freeze and thaw from the ground surface and downwards, with the uppermost part of the active layer freezing and thawing approximately two months before the deepest parts. In July and August the response to rain and evapotranspiration is clear in the upper soil profile (10 cm and 20 cm). The rains in August saturated the soil profile and this high water content remains until freezing in November. As with the soil temperatures the response to precipitation is much more pronounced close to the soil surface.

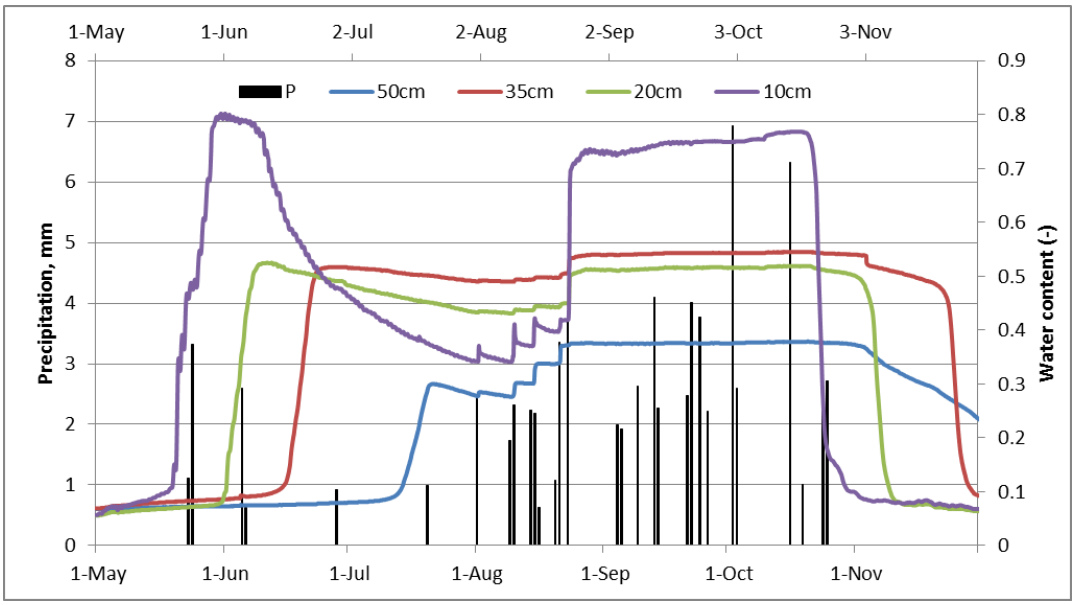

Figure 14. *Soil moisture data at 10, 20, 35 and 50 cm depth co-plotted with precipitation.*

Lysimeter transects

In August 2011, soil lysimeters were installed in three transects, each with two or five locations (Fig. 19). At each location, two to five lysimeters – installed at approximately every 10 cm starting from 10 cm below the soil surface – form a depth profile down to the permafrost at about 35 to 70 cm soil depth (Fig. 13 and 15). Lysimeters were installed at the same sites as the time-domain reflectometer instruments that were used to measure soil water content in the hydrological studies described above.

Figure 15. *Lysimeter and TDR installations in the active layer. To the right: lysimeter flasks with soil water ready to collect.*

Lake oxygen and temperature

Results from the in situ measurements of dissolved oxygen and temperature (Fig. 16) show the highest oxygen concentrations in the end of the autumn. During winter, a sharp decrease in dissolved oxygen is observed at 17–20m depth, whereas the oxygen level at 5–8m depth is relatively stable the whole winter period. During summer the oxygen concentrations decrease slightly both at shallow and greater depths as the lake temperature rises (Lindborg et al. 2016).

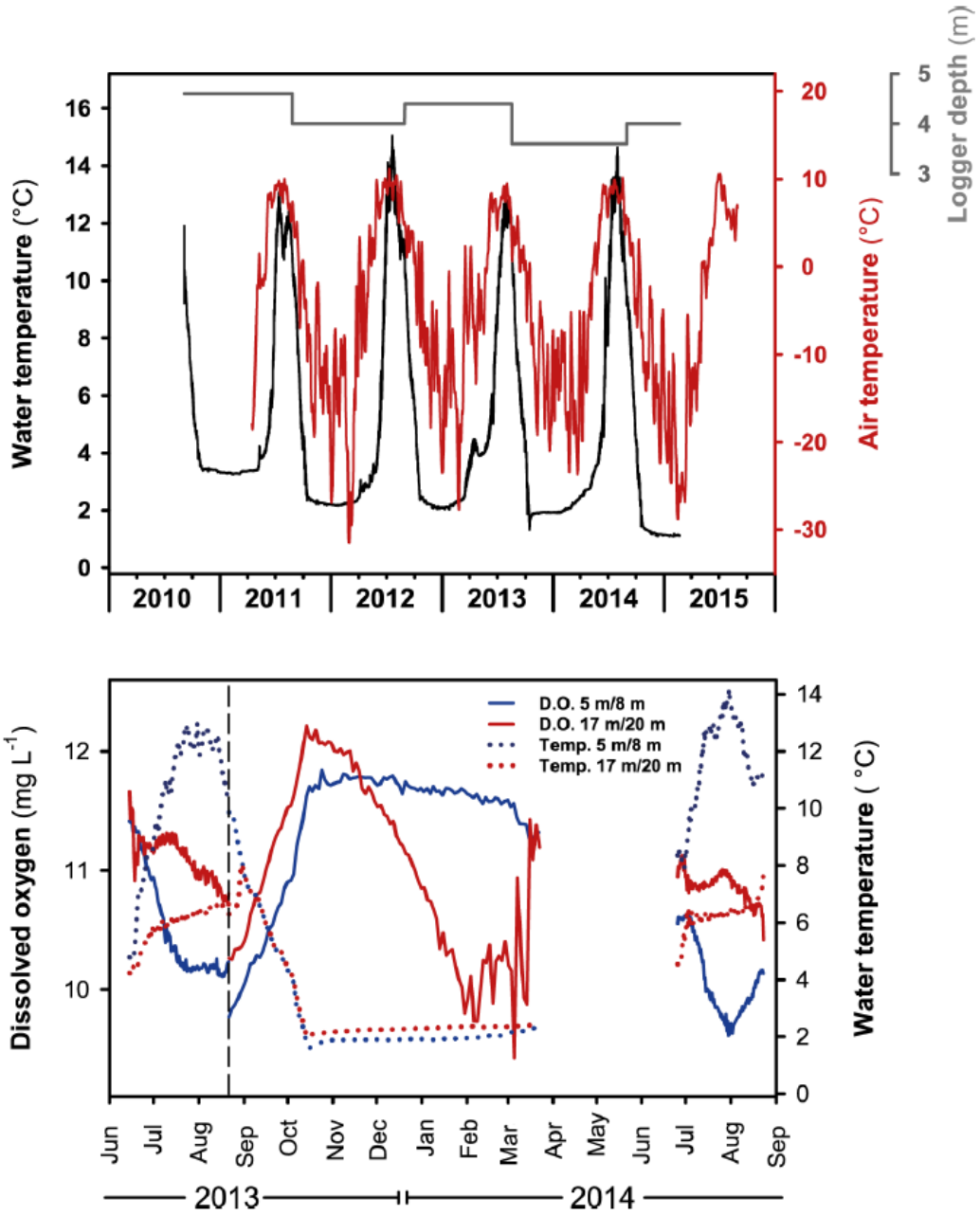

Figure 16. *Upper figure: graph displaying the variations in lake water temperature at about 4m water depth and air temperature during the period from 2011 to 2015. Lower figure: graph displaying the variations in dissolved oxygen and temperature during measurements in 2013 and 2014. From Lindborg et al. (2016).*

Time lapse cameras

Three time lapse cameras were installed in August 2012 at different locations within the catchment with the purposes of monitoring hydrological events during the year and to support interpretations of the quantitative time series obtained from the AWS. The time lapse camera installations provides very useful information for mapping local temporal variability in ponded water or snow cover, to validate the snow models developed for the catchment and to determine the timing of ice-in and ice-out. One camera is placed to give an overview of the whole catchment; one is placed to monitor details of hillslopes and one camera monitor the surface water inflow to the lake. Photos were taken every second hour, see figure 17 for example pictures.

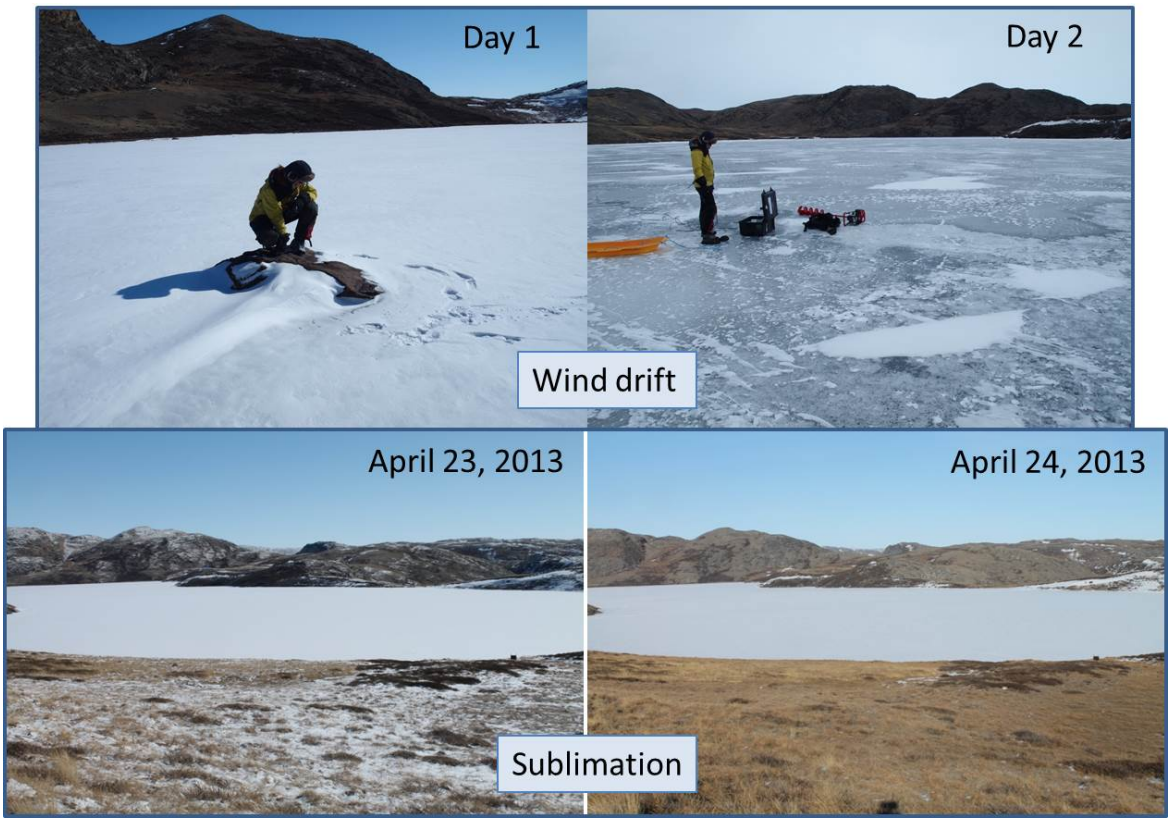

Figure 17. *Time lapse photos showing examples of snow drift event (upper figure) and sublimation (lower figure). During both events negative temperatures (°C) were recorded, i.e. no snow melt occurred.*

Sampling of water, soil, sediment and biota at TBL

The overall study design and data collection protocol for TBL were based on a conceptual model describing the different functional units of the ecosystem (Fig. 18). The idea is to combine the data on elemental concentrations for the different components of the ecosystem with the hydrological model (Johansson et al., 2015b) and geometrical information (Petrone et al., 2016) in order to develop our understanding on both pools and fluxes in the TBL-catchment. The pools and fluxes are then used to develop numerical models describing the transport and accumulation of various elements on a catchment scale. In Figure 19 the sampling locations are shown within the TBL catchment.

Work presented herein is therefore an attempt to capture the broad picture of element behavior at the catchment scale in a mass balance model. In principle, the mass-balance model can be broken down into four main compartments: the seasonally unfrozen terrestrial system (active layer), the permafrost, the lake water, and the lake sediments, which can be further separated into separate pools. The inputs to the system occur as wet deposition (precipitation) and eolian deposition, whereas eolian erosion in the terrestrial area and outflow (via the lake outlet and through the talik) accounts for the export from the system. Internal fluxes between pools can be both uni- and bidirectional, and include, e.g., the transfer of material to the permafrost, runoff to the lake and burial in the sediment. These internal fluxes result in changes in the storage of elements within the different pools.

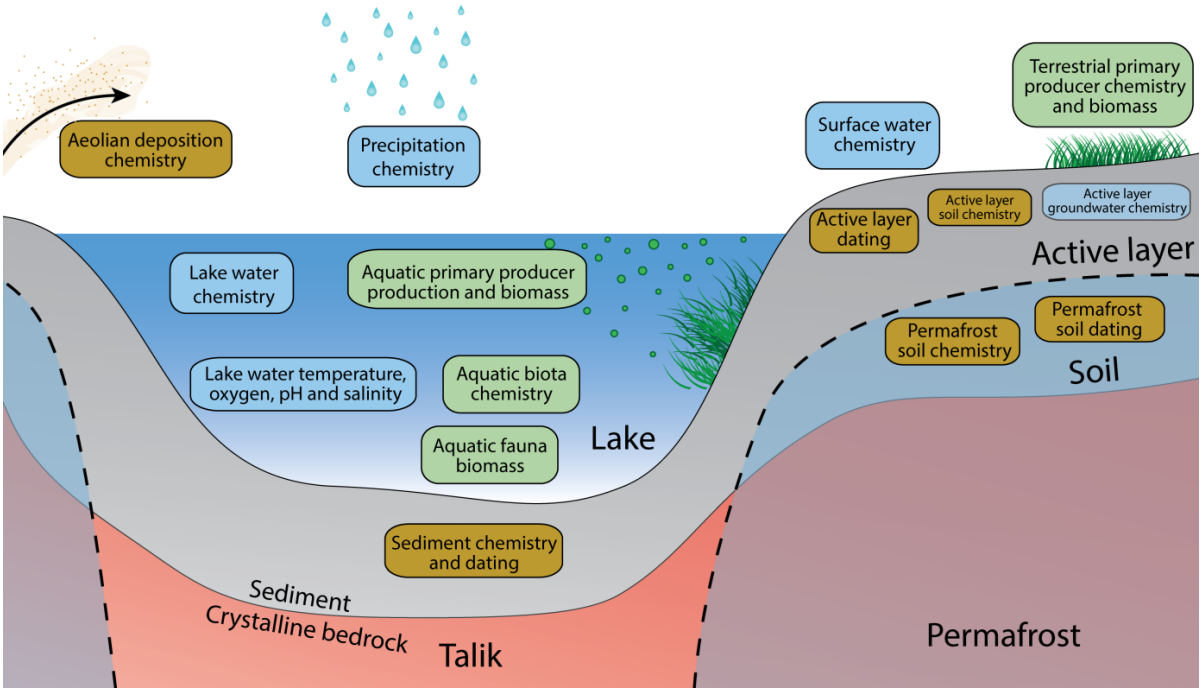

Figure 18. *Conceptual model of the TBL catchment describing major ecosystem entities (boxes) in the landscape. Boxes are divided into water (blue), biotic (green) and solid matter (brown). Figure from Lindborg et al. (2016).*

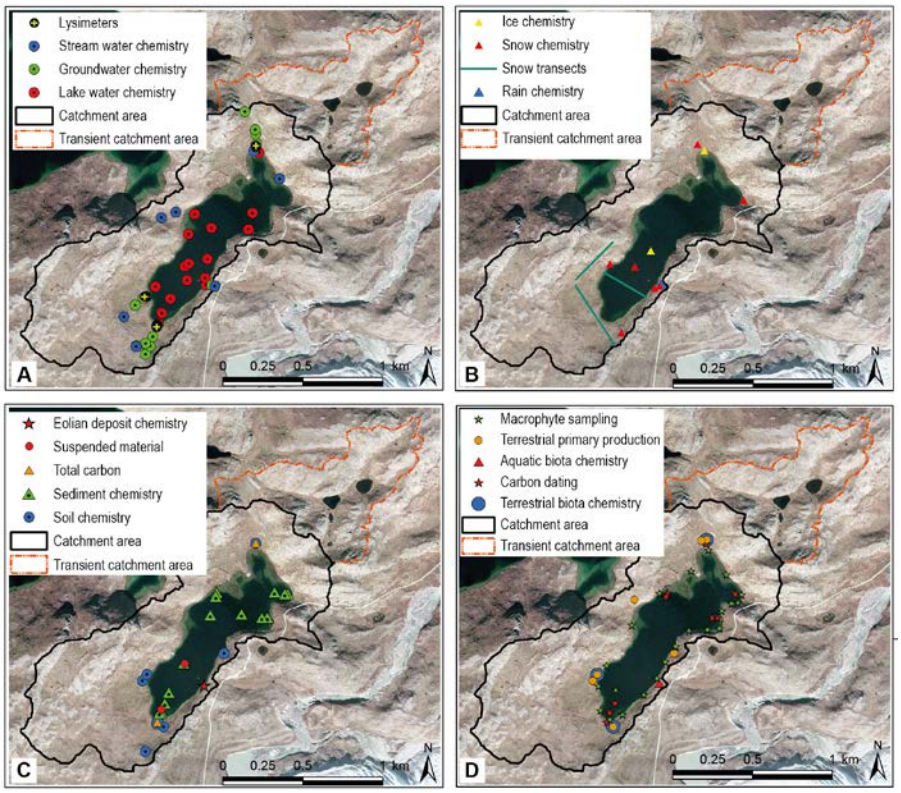

Figure 19. *Map of the TBL catchment and sampling points. A) water sampling B) precipitation and ice sampling, C) Soil and sediment sampling and D) biotic sampling. In dotted orange is a transient catchment active during spring thaw. Modified from Lindborg et al. (2016).*

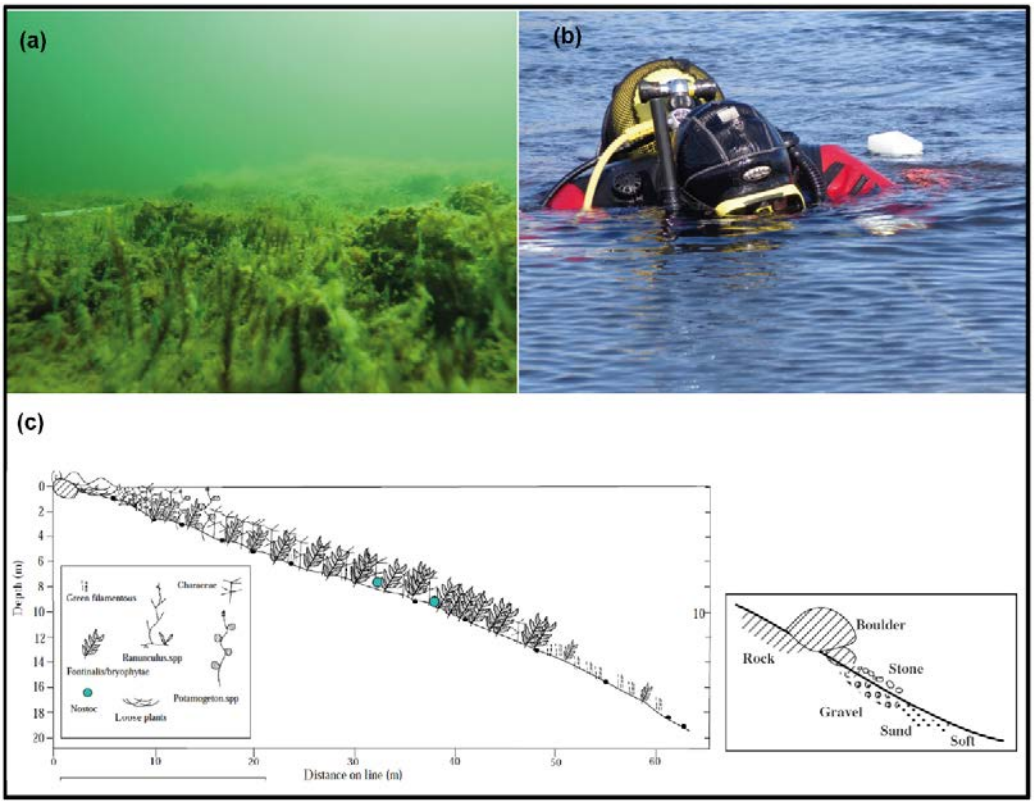

Figure 20. *Dive transect for macrophyte and lake bottom substrate inventory. From Lindborg et al. (2016).*

Figure 21. *Vegetation types found in the Two Boat Lake catchment. Gross primary production, respiration and soil organic matter content were determined for each type. Photographs taken in late June 2014.*

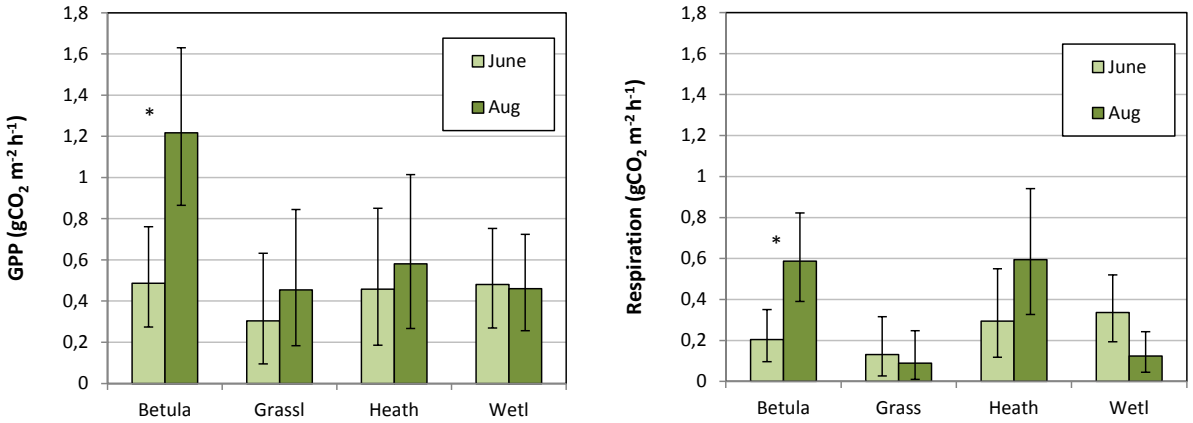

Figure 22. *Gross primary production (left) and respiration (right) in four vegetation types measured in late June and mid-August. Least square means (bars) and standard error (whiskers) are given. Asterix indicate a significant difference between seasons (p<0.05).*

Terrestrial vegetation and top soils

During the summers of 2013 (mid-August) and 2014 (late June) gross primary production and respiration were estimated in four vegetation types (Fig. 21). The birch shrub (Betula) and wetland types were represented by two locations, whereas the grass and heat types were represented by one location each. CO_2 fluxes (in light and darkness) were measured at fixed sampling points within each location, using a canopy assimilation chamber (CPY-2, PP Systems,

Hitchin Hertfordshire UK) attached to an infra-red gas analyzer (environmental gas monitor EGM-4; PP Systems). During the 2014 campaign, the top soil (12 cm) in each vegetation type was also sampled (Lindborg et al. 2016). For each location two soil cores were taken, and the soil within each core was divided into four 3 cm sections. Roots were removed by sieving (<2mm), and loss on ignition of all soil samples were determined by combustion at 550 °C. The geochemical composition of soil and vegetation samples was determined through ICP-MS analysis. Gross primary production (GPP) was positively correlated to photosynthetic active radiation (PAR, p=0.05), but varied little over the season for most vegetation types (as compared to the between location variation; Figure 22). Betula shrubs were an exception to this pattern, as GPP was significantly larger in August than in June. The patterns of respiration followed those of GPP, and there was no overall decrease in August, even though the average temperature was 3 °C degrees lower than in July. However, in wetlands there was a tendency that respiration decreased in August, possibly indicating that the contribution of heterotroph respiration was more important in this system. The content of organic carbon clearly decreased with depth in the top soil (Fig. 23). The average concentration was lower in grassland than under shrub, heath and wetland vegetation. However, the spatial variation in wetlands was substantial. The highest amount of accumulated carbon was found in the northern wetland location, which had more than twice as much organic matter as the other locations in the lower half of the soil cores (soil core in Figure 21). According to a principal components analysis (PCA) based on the geochemical data for all solid samples (biota, soils and lake sediments), the solid samples fall into three different groups (Fig. 24). All soil samples have high scores for both principal component (PC) 1 and PC-2 indicating high concentrations in lithogenic elements (Zr, Si, Ti, Al, etc.). The lake sediment samples have intermediate scores for PC-1, indicating that they contain a mix of biological and minerogenic material, and high scores for PC-2, which suggest a higher content of degraded organic material rich in bromine and sulfur. The biological samples, both from aquatic and terrestrial system, have low scores on both PC-1 and PC-2 indicating that they do not contain any minerogenic material and consists of fresh organic material.

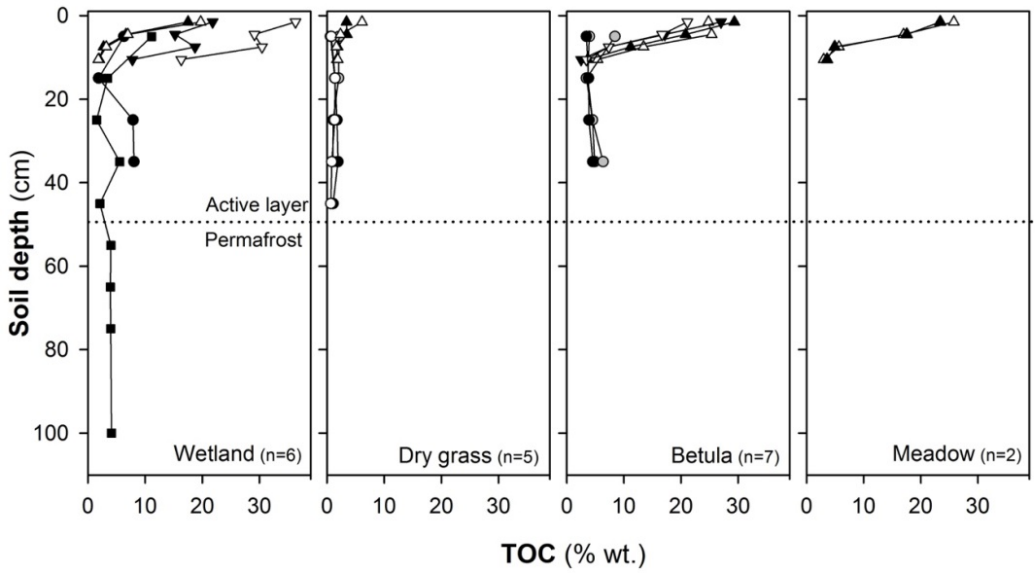

Figure 23. *Soil organic matter content (measured as % organic carbon) as a function of soil depth in four vegetation communities.*

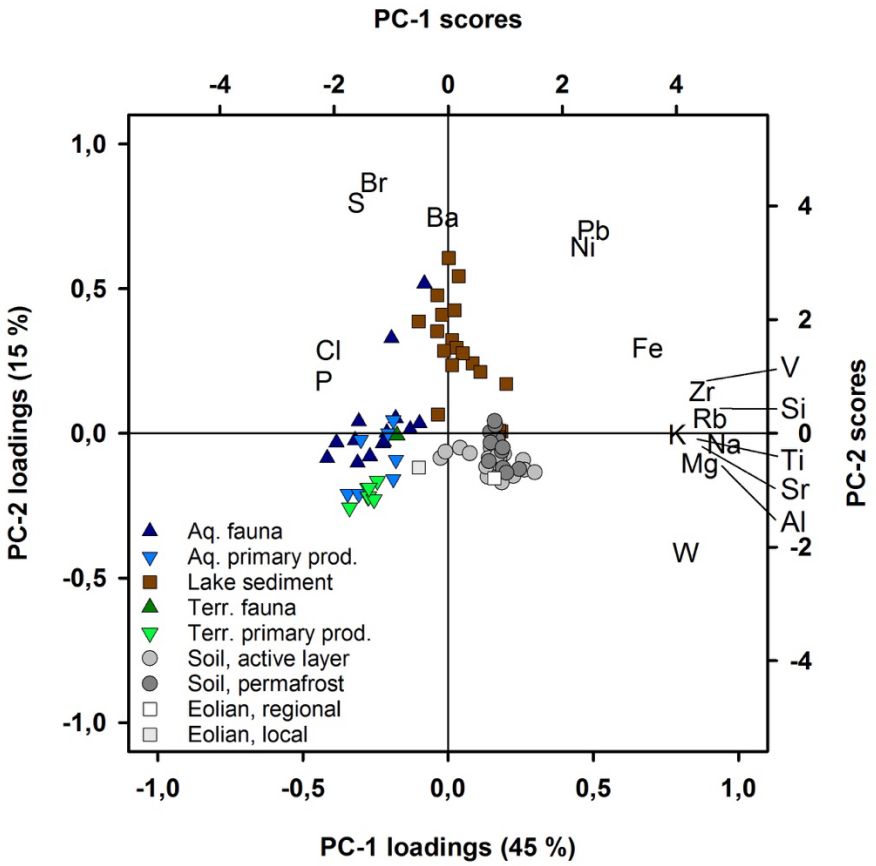

Figure 24. *A combined loadings and score plot describing the similarities and differences in the geochemical composition of all solid samples collected from the TBL-catchment.*

Precipitation, soil water and lake water

The concentration of organic carbon (TOC/DOC), nitrogen and phosphorus in precipitation is highly variable (Fig. 25), with old snow samples having much higher concentrations than fresh snow, which contain virtually no TOC/DOC, nitrogen or phosphorus. Lake-water samples generally have lower concentrations of TOC/DOC, nitrogen and phosphorus as compared to soil water (lysimeters) and surface water (groundwater wells and temporary streams), but higher concentrations of dissolved inorganic carbon (DIC: Fig. 25)). When looking at the geochemical composition using PCA it is clear that precipitation samples are low in both elements released by weathering (PC-1) and enriched by evaporation (PC-2; Fig. 26). Lake water samples have similar concentrations as precipitation for elements associated with weathering, but are much higher in elements that are enriched by evaporation. The soil water samples show a large degree of variability, but especially the lysimeter samples generally have higher concentrations in elements released by weathering.

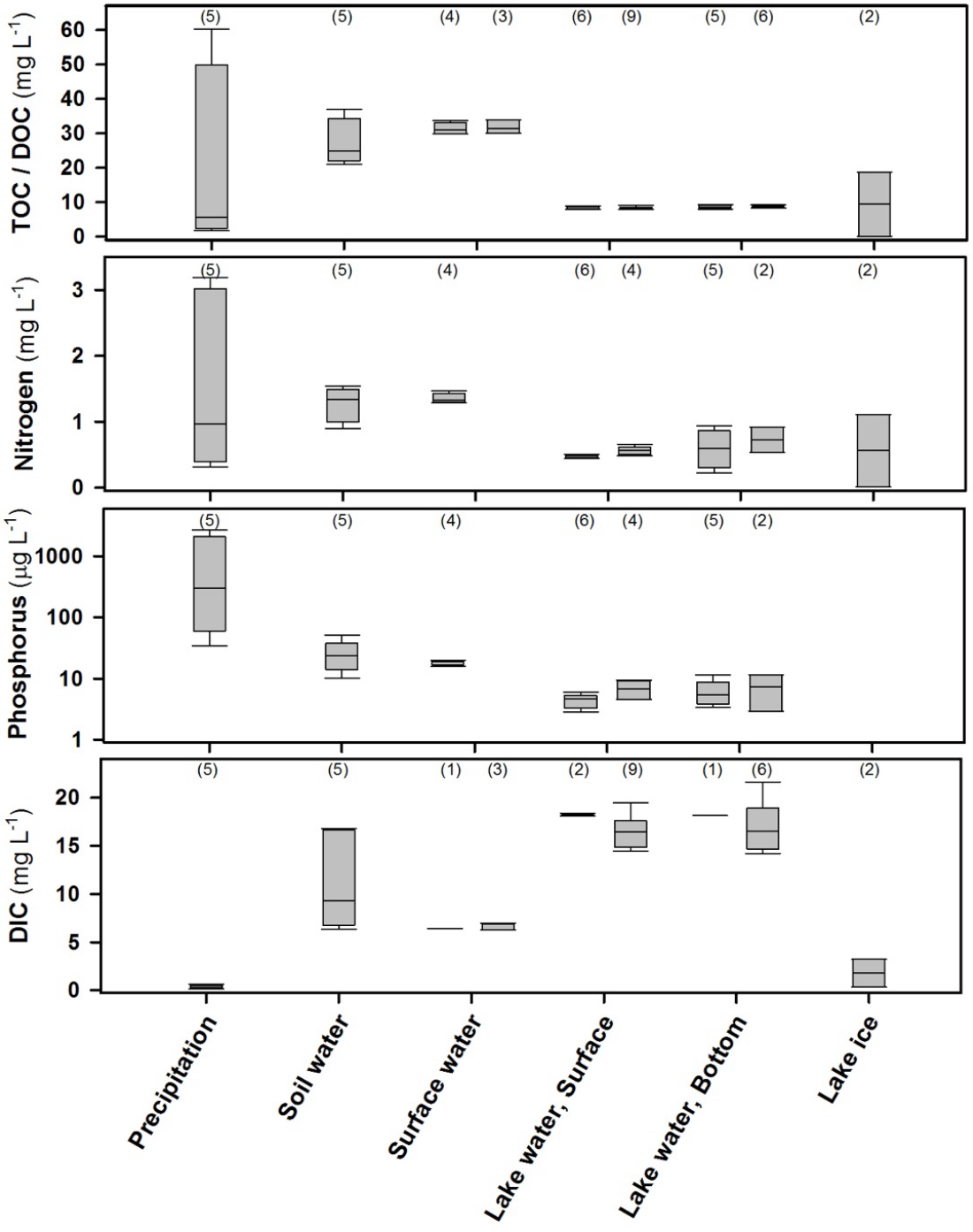

Figure 25. *Box plot showing the range of concentrations for organic carbon (TOC/DOC), nitrogen, phosphorus and dissolved inorganic carbon (DIC) in water samples from the TBL-catchment.*

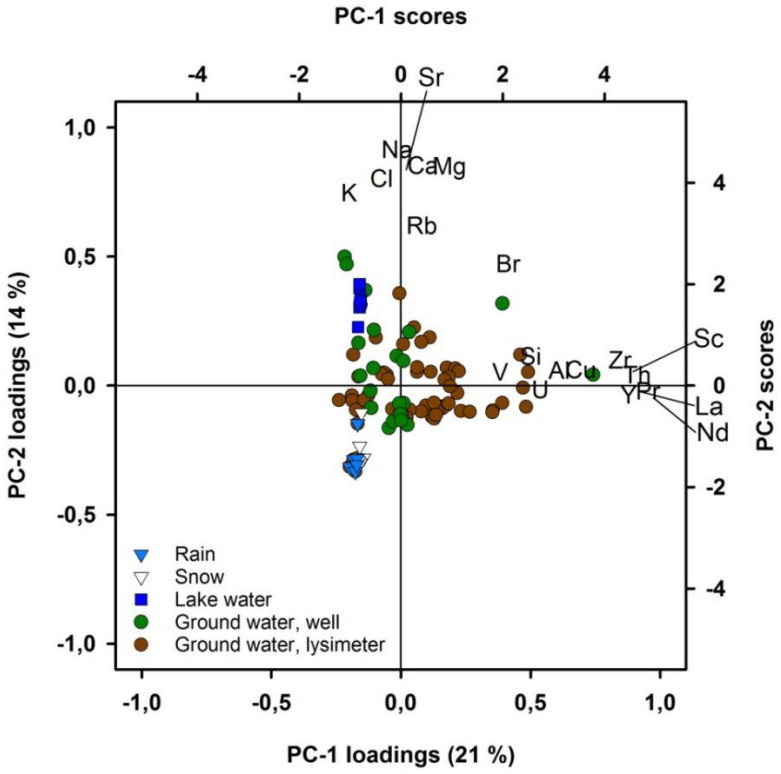

Figure 26. *A combined loadings and score plot describing the similarities and differences in the geochemical composition of all water samples collected from the TBL-catchment. High PC 1 scores represent high concentrations in elements released by weathering, while high PC 2 scores represent high concentrations in elements enriched by evaporation.*

Lake sediments

Lake sediments have been sampled on several occasions. A long sediment profile from the deepest part of the lake was collected in 2011. This profile was used by Rydberg et al. (2016) to study the long-term history of the lake through its geochemistry (Fig. 27). The sediment quality is highly variable and the profile can be divided into three separate phases. An initial phase with relatively high sediment accumulation rate and lower organic matter concentrations. The second phase is represented by a 1-cm thick clay layer, which indicate that a sudden event have occurred in the catchment. From the present data it is not possible to determine what caused this clay layer, but it is obvious that the sedimentation rate in the last phase is lower as compared to during the first phase. The third phase also generally have higher organic matter concentrations, even if the lower sediment accumulation rate actually means that less carbon per year is buried in the sediment during phase three than during phase one. One important driver for the sediment geochemistry seems to be eolian deposition. PC-2 – which relates to the zirconium (Zr) concentration, and where more Zr represent a coarser grainsize – shows two periods with coarser material (lower scores). The periods with lower PC-2 scores fit well with other records of eolian deposition (Fig. 27). In 2012 a number of short sediment cores were collected from various locations in TBL (Figure 28). The rational for this was to assess the accumulation of carbon and other elements in the entire basin. As expected, there are considerable variability in both the appearance and sediment composition between locations (Fig. 29 and 30). Shallower locations – where the sediment is covered with mosses and aquatic macrophytes – have considerable higher carbon concentrations (Fig. 30). For iron the spatial variability is even higher, with cores collected from about 17-m water depth having much higher iron concentrations as a result of redox processes within the sediment leading to the in-situ formation of iron precipitates (Fig. 30).

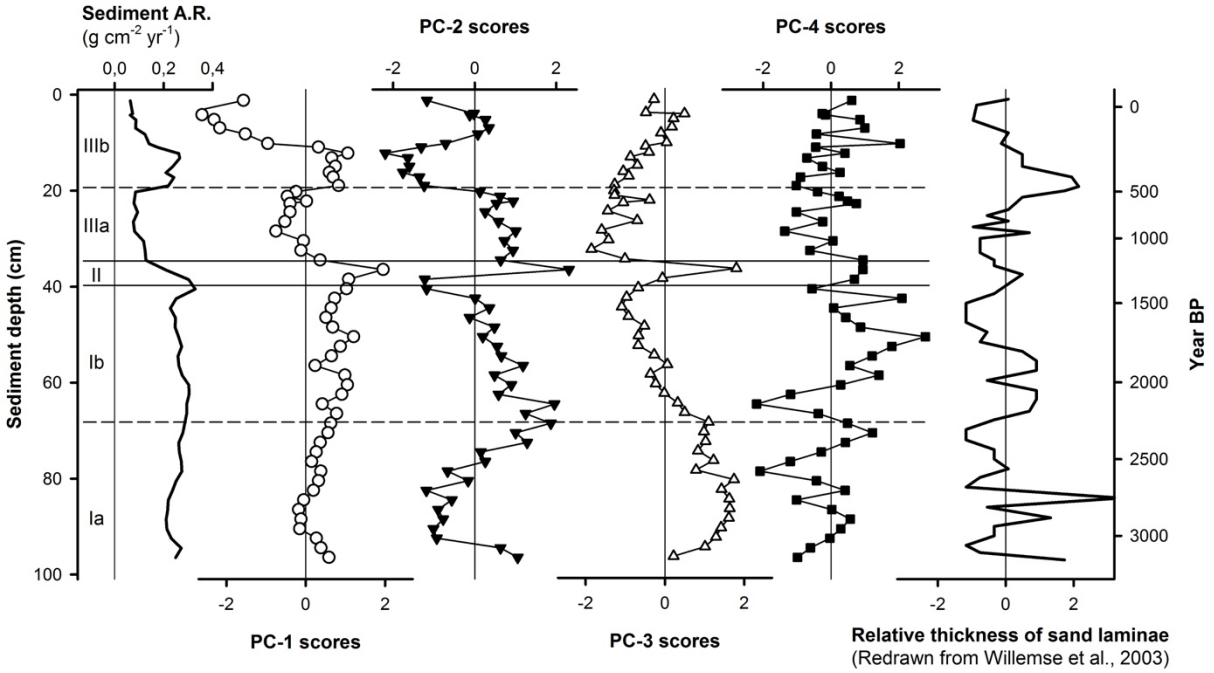

Figure 27. *Data from the long profile collected in the deepest part of the lake. The record spans most of the lakes history, and shows considerable changes in both sediment accumulation rate and the sediments geochemical composition. The first PC (PC 1) represent changes in the amount of organic carbon in the sediment (low scores = more carbon), while the second PC (PC 2) represent the grainsize (lower scores indicate lower concentrations of zirconium, and thus a coarser grainsize). The variation in grain size is driven by variations in eolian deposition (see the panel to the right), with more eolian activity resulting in a coarser grainsize in the sediments of TBL.*

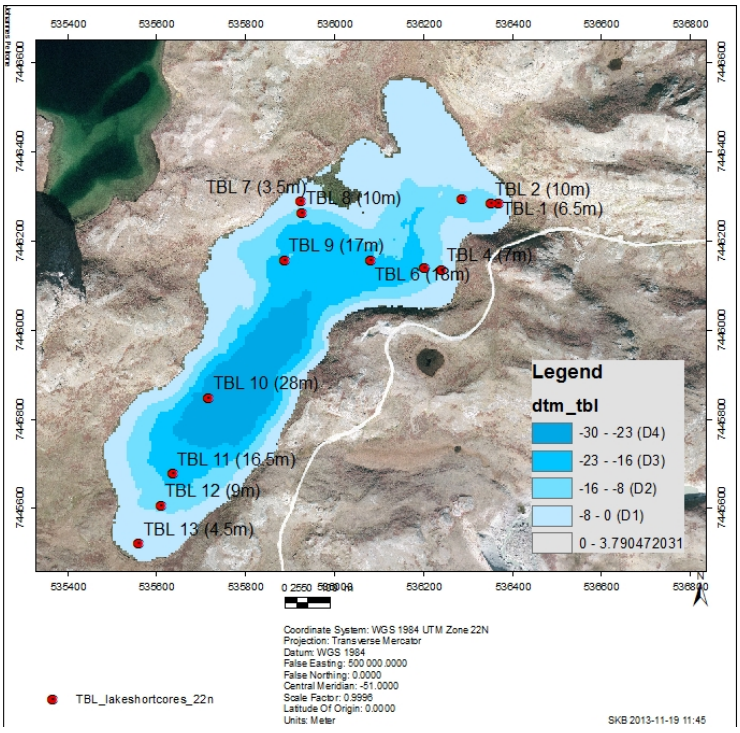

Figure 28. *Sampling locations for the 13 short sediment cores collected from TBL in 2012.*

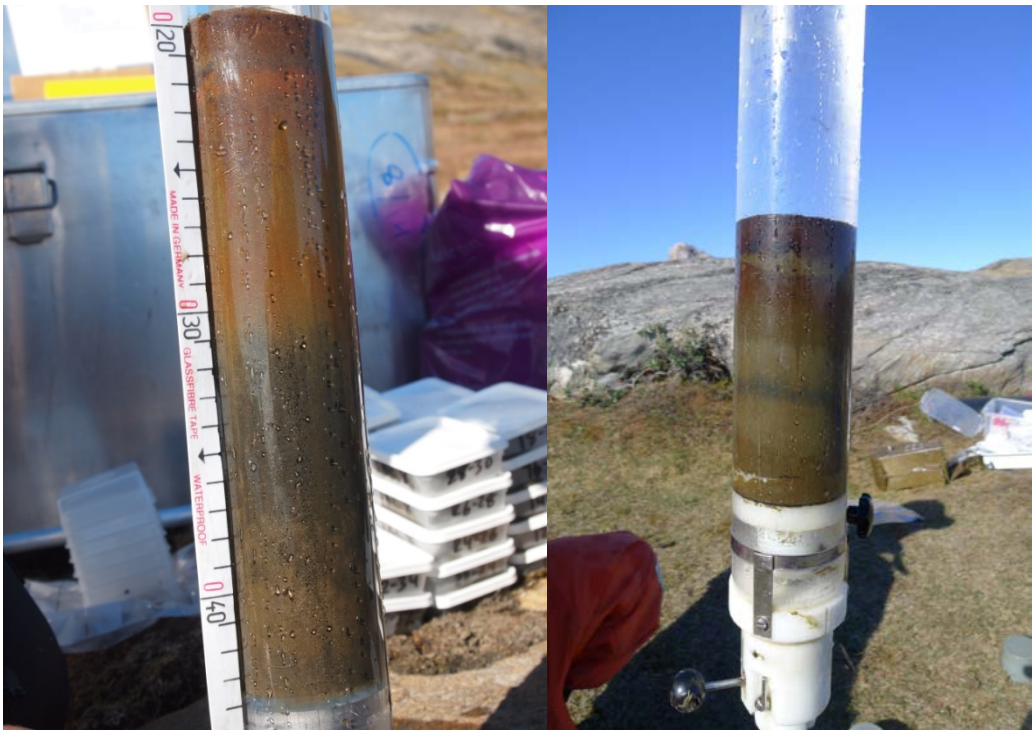

Figure 29. *Sediment cores from TBL. Distinct lamination that relates to changes in sediment composition can be seen in both cores. The left photo shows the TBL-9 core collected at 17-m water depth, while the photo on the right shows a core collected in 2011 in the deepest part of the lake (i.e., 28 m).*

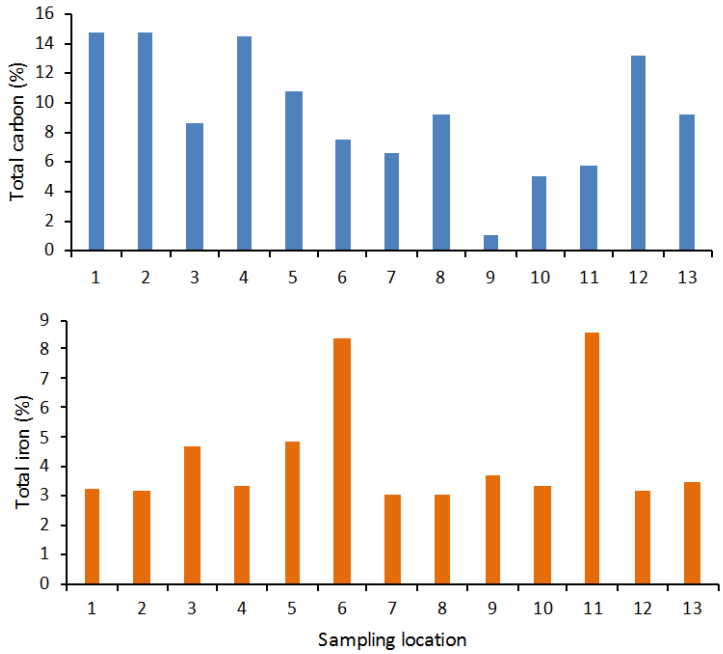

Figure 30. *Total carbon and total iron concentrations of the 13 short sediment cores that were collected in 2012. Total carbon is higher in the cores collected in shallower depths as compared to those collected from deeper areas. This can largely be attributed to the presence of mosses and other aquatic vegetation at depths down to about 14 m. For total iron, cores collected at depths from around 17 m have higher concentrations in the surface layers. This is related to redox processes causing an enrichment of iron at boundary between oxic and anoxic conditions (see also the photo of the TBL-9 core in Figure 29, where the red-orange colour is a result of the presence of ironhydroxides and oxyhydroxides in the sediment).*

Maps describing the TBL catchment

Vegetation

The construction of the vegetation map was done by delineation of areas with uniform appearance in aerial photographs as individual polygons, and these polygons were grouped in classes based on comparable qualities as appearing in the photos. The result was a polygon mosaic where the identity of the classes was largely unknown. Polygons representative for each class were examined in the field, whereby the classes were given descriptive names (Fig. 31). We did not, at this stage, perform quantitative investigations of plants species densities. All field investigations were based on inventory of occurrence and visual estimates of ground coverage of each species. Some of the classes that resulted from remote sensing interpretation were merged into a common class, when examination in the field revealed it as a negligible difference in density of a certain species. However, when density differences were large enough to make up discernible boundaries in the field, classes were kept as interpreted by remote sensing.

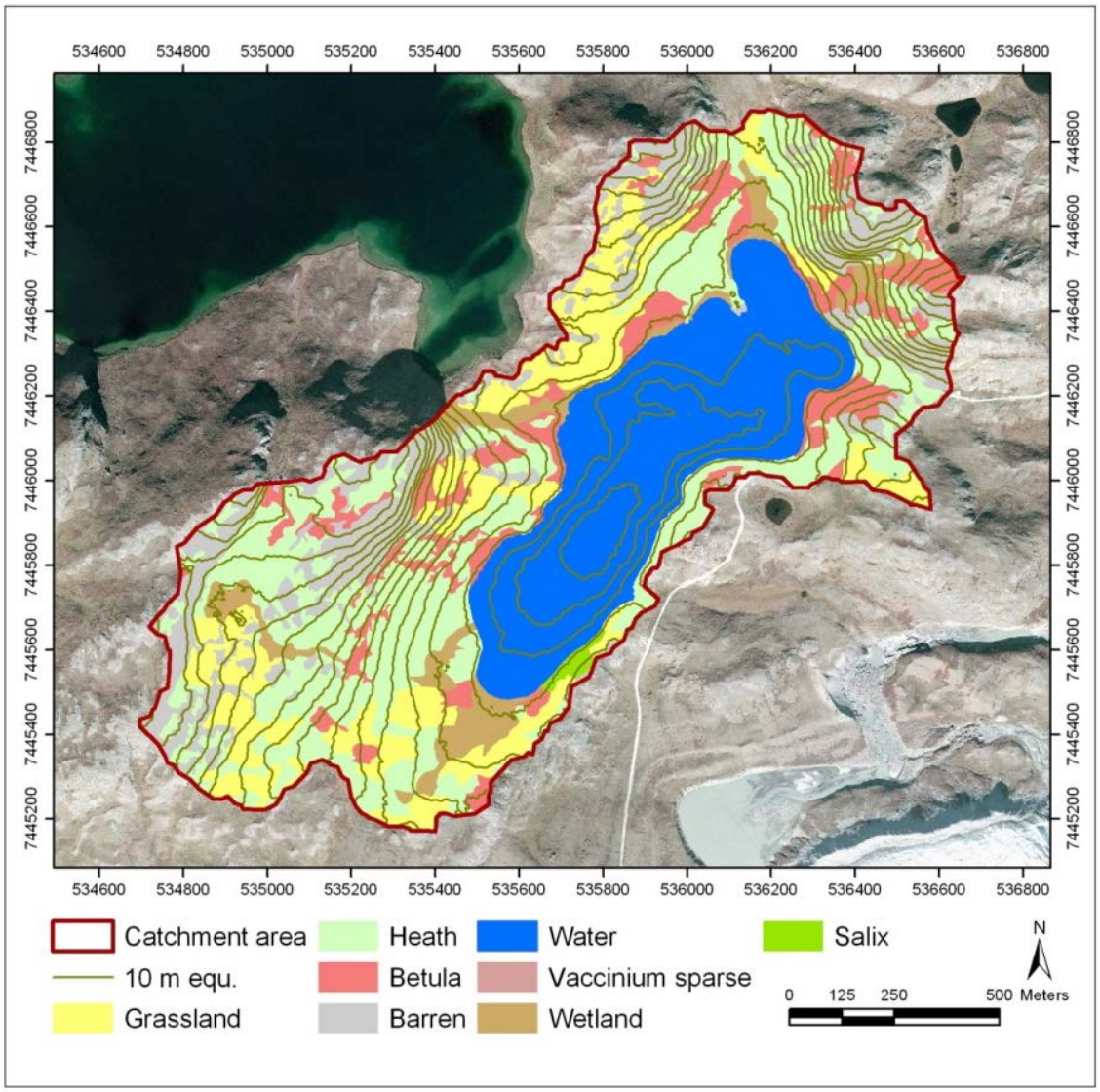

Figure 31. *Vegetation map of TBL catchment. From Petrone et al. (2016).*

Quaternary geology and active layer thickness

A Quaternary geology map (Fig. 32), based on results from excavations and field observations, is presented in Petrone et al. (2016). The uppermost sediments are dominated by eolian silt, underlain by till, which is also representative of the regional area. Deposition of the eolian silt has occurred since at least ca. 4750 years BP, when the ice margin was situated further inland. Surficial glacial till and bedrock outcrops can be found in places where erosion has removed the eolian silt. The boundary is often sharp with a scarred surface revealing the underlying till. The till is loosely compacted and is dominated by sand and gravel with a low content of silt and clay, which indicates a marginal deposition in front of the ice sheet. Glaciofluvial deposits are also found in several areas, mainly in the northern regions of the catchment. Stratigraphical studies have shown that the till contains layers of water laid deposits and the hydrological properties of the till and the glaciofluvial deposits can therefore be regarded as comparable. In the central and low-lying parts of the major valleys, silt deposition and accumulation of organic material have resulted in areas of peaty silt. The floor of the lake is covered to a large extent by currently accumulating silt. Permafrost-related processes have also led to the development of ice-wedge polygons in local areas where the sediments are characterized by relatively high water content.

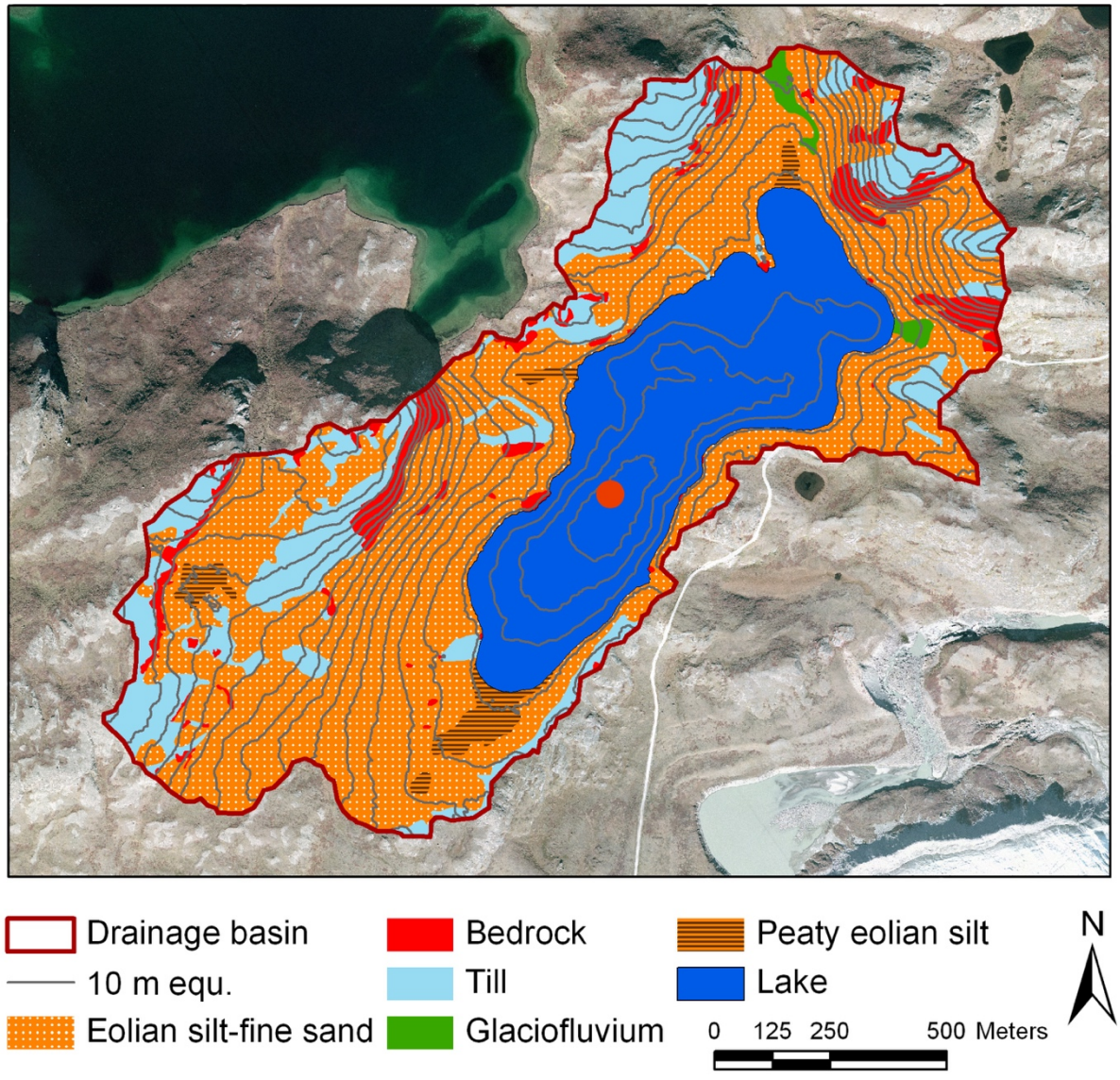

Figure 32. *Map showing soil type distribution in the Two Boat Lake catchment. From Petrone et al.(2016).*

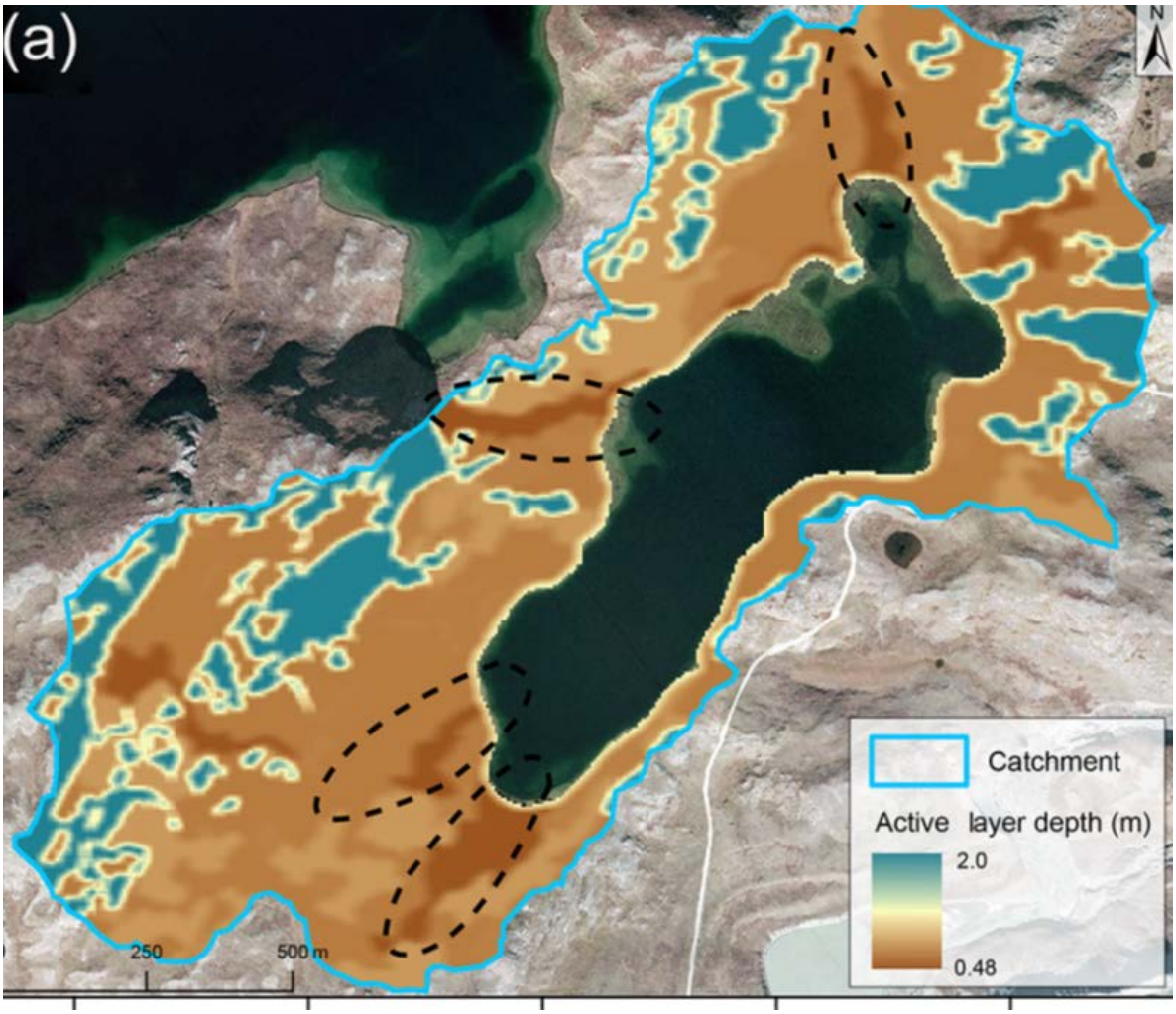

Figure 33. *Active layer depth model.*

In order to calculate the depth of the active layer it was necessary to know the wave velocity in the medium. Eolian silt covers a major part of the catchment, and it is considered homogeneous down to the underlying till. Thus, mainly water content and organic matter varies in the sediment layer, hosting the active layer. The variation in vegetation within the study area can therefore be correlated to soil water content. In Petrone et al. (2016) a thorough description is made on methods, results and implications on upscaling of results.

Hydrology

Based on data from the TBL catchment the main hydrological flow paths within and across the catchment boundaries of TBL was identified and quantified by constructing a hydrological conceptual and a numerical (Fig. 35). During the active period, three runoff components are defined in the conceptual model (Fig. 35): surface water flow to and from the lake (R_s) and groundwater exchange between the lake and the active layer (R_{al}) and via the talik (R_{gw}). During the frozen period R_s and R_{al} are zero. Due to the non-frozen conditions in the talik R_{gw} is non-zero also under the frozen period. During winter, sublimation and snow drift is shown to be important processes and mass loss via sublimation influences the catchment water balance. The groundwater exchange with the talik (R_{gw}), which is concluded to be directed downwards, constitutes only 6% of the annual inflow of water to the lake (R_{al}+R_s).

Overall, the water balance (Fig. 34) for the investigated period is dominated by the evapotranspiration component, being almost equal to the precipitation input. No surface water outflow has been observed from the lake since the site investigation started. 2011 is shown to be a historically dry year with a low lake level as a consequence. The lake level is still recovering from this dry year. However, the simulations of different weather conditions, based on the available long-term time series from the settlement of Kangerlussuaq, adjusted to the local conditions at the TBL site, indicate a positive water balance with surface water flowing out from the catchment under normal weather conditions (Fig. 34 right). This is also confirmed by isotopic analysis of groundwater levels in the active layer downstream the lake having the same isotopic signature as the lake water. The long term water balance under normal weather conditions for the catchment is P 369 mm, ET 258 mm and R 11 mm where R is divided into surface runoff of 7 mm and groundwater recharge to the talik of 4 mm.

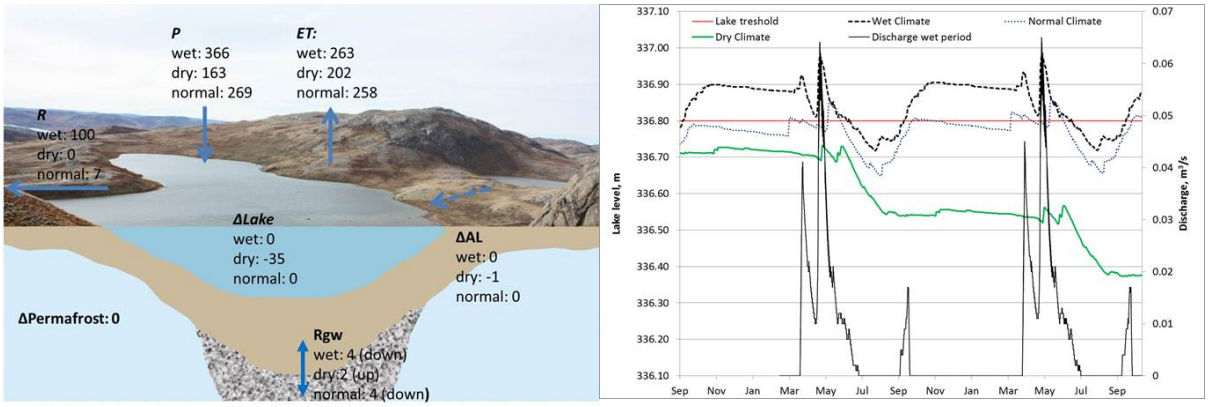

***Figure 34**. The overall water balance for wet, dry and normal weather conditions in the TBL catchment (left). In the right figure the lake water level for each weather condition is plotted together with the surface run off from the catchment.*

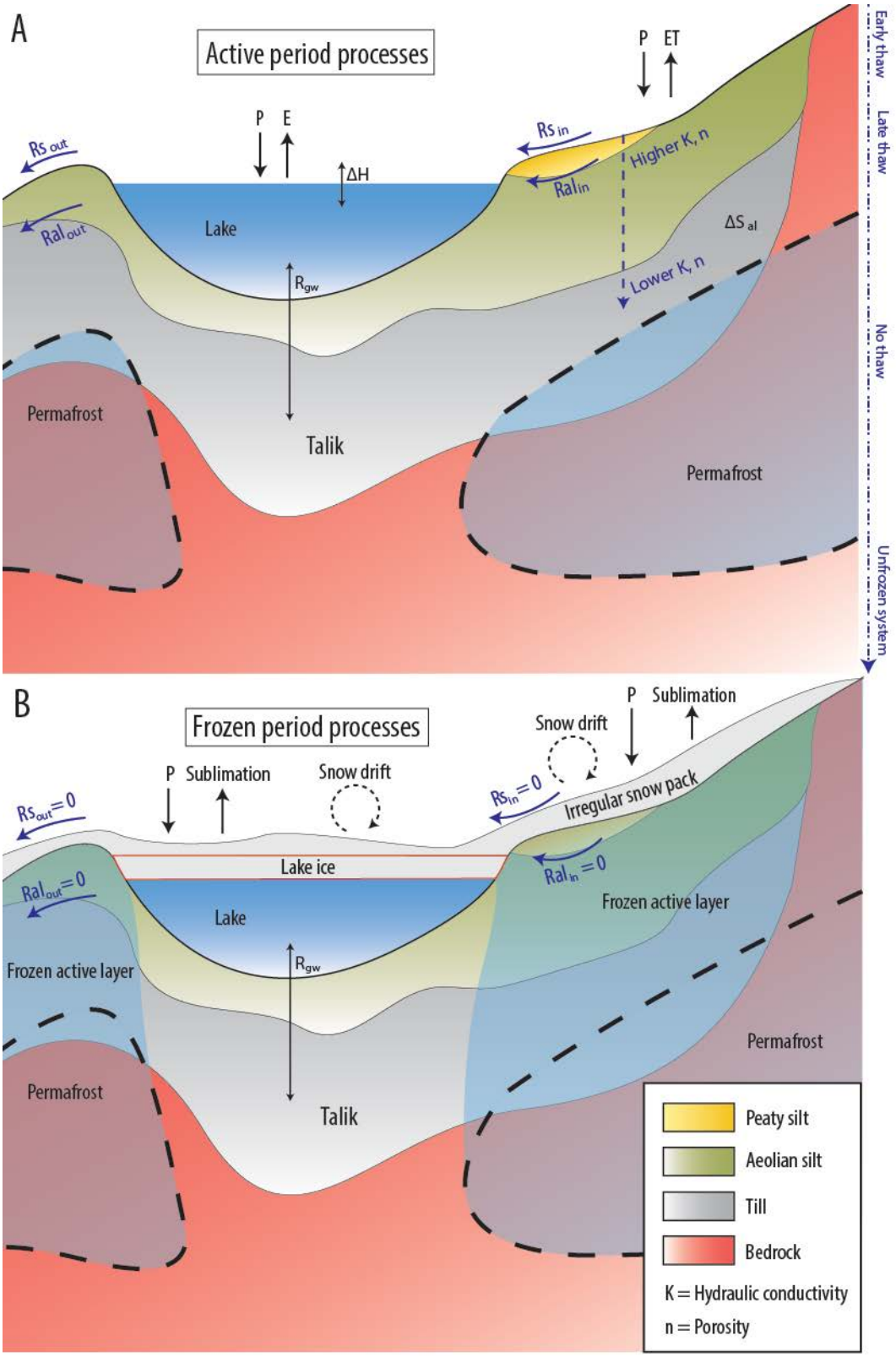

Figure 35. *Conceptual model describing runoff components at TBL for, A: active period, B: frozen period.*

TBL ecosystems and mass balances

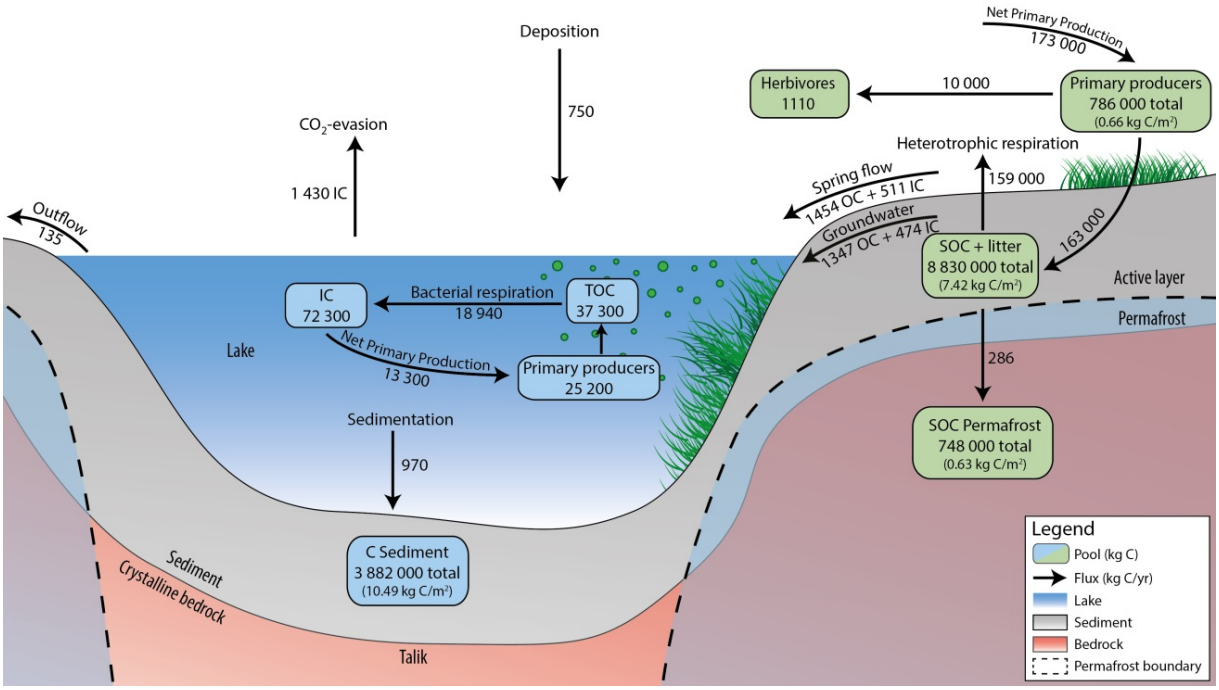

Figure 36. *Carbon mass-balance model of the TBL catchment. Manuscript submitted, Lindborg et al.*

A carbon mass-balance budget for a periglacial catchment situated in West Greenland close to the Greenland ice sheet has been constructed. The mass balance budget is obtained by investigating both biotic and abiotic properties, quantifying the major carbon fluxes and pools, and linking the terrestrial and aquatic parts of the catchment. Overall there is a small positive imbalance (less than 1 % of the inputs) in the carbon mass-balance budget for the entire TBL catchment, which indicates that, even if many flux estimates are associated with large uncertainties, our carbon mass-balance budget realistically describes the carbon cycling in the TBL catchment. The largest carbon pools are the soil active layer (61%) and the lake sediments (27%). Only 5% of the catchment carbon pool is found in the permafrost. The main input of carbon in the TBL catchment is terrestrial net primary production, and the main export occurs as soil respiration. Even if the transport of carbon from the terrestrial to aquatic system is smaller than in other wetter areas, the input of 4500 kg of terrestrial carbon each year plays an important role in supporting the aquatic carbon cycle. The negligible C yr-1 n this dry landscape (mean annual precipitation is 173 mm) with a limited hydrological transport of carbon from the terrestrial to the aquatic system, the aquatic system is heterotrophic and the main export of carbon from the aquatic system is through CO2-evasion. Riverine export is almost negligible. Our data also shows that 3-4 times more carbon is buried in the sediments than is incorporated in permafrost soils. Above text slightly modified after Lindborg (2017).

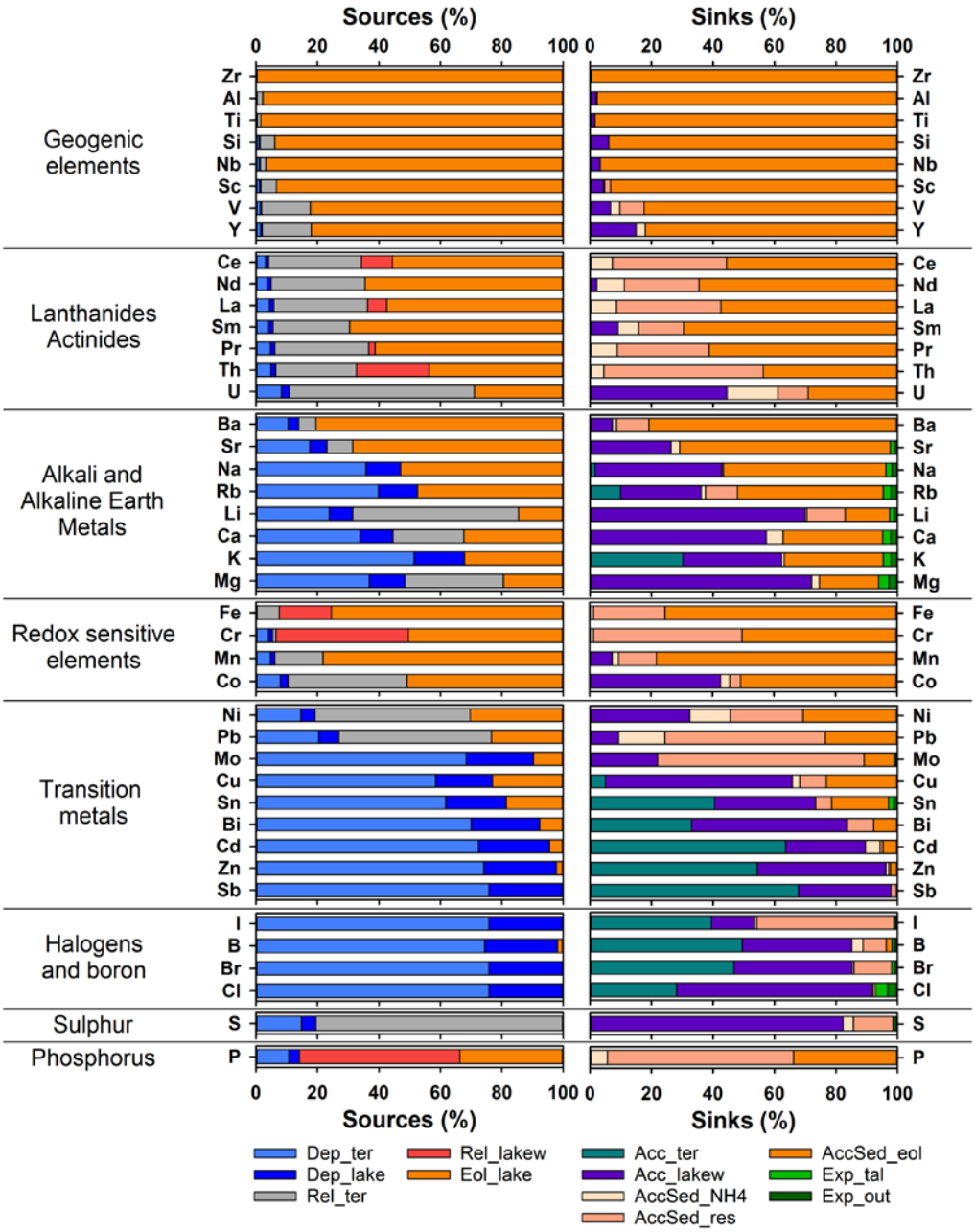

Figure 37. *Element fluxes in the TBL catchment.*

Other elemental fluxes: In a mass-balance model eight element groups were identified based on their common origin and/or behavior (Fig. 37). Here follows a brief description of these groups and the processes behind the observed patterns. From Lindborg (2017).

The *Geogenic elements* comprise Zr, Al, Ti, Si, Nb, Sc, V and Y, which are all strongly related to minerals and for which eolian transport is the main source. In the terrestrial landscape weathering of these elements (represented by Rel_ter) is generally low, with slightly higher release to pore waters for Sc, Si, V and Y as compared to Zr and Ti. The residual Acc_Lakew indicates a slight build-up of these elements in the lake water, but the positive balancing term could also be related to uncertainties in the data.

The *Lanthanides and actinides* comprise Ce, Nd, La, Sm, Pr, Th and U. Similar to the *Geogenic elements*, the main source is eolian deposition, but unlike the previous group there is a part of

the sediment accumulation that cannot be explained by the eolian input. Most of this discrepancy can be accounted for by weathering in the terrestrial system, but for some elements (Ce, La, Pr, Th) the mass-balance model indicates an unknown source (AccSed_res), and it should be noted that these elements are only analysed in one of the sediment cores. For U there is also a relatively large accumulation in the lake water. Thermodynamic modelling of the lake water suggested that this possibly could be related to formation of soluble carbonate complexes.

The group *Alkali and alkaline earth metals* contains Rb, K, Na, Li, Ba, Sr, Ca and Mg that all have several important sources. The biggest difference from the previous groups is that atmospheric deposition was a much more prominent source (for Ca, Mg and Rb it was even the most important source), but there is still an important contribution from eolian input for most of these elements (except Li and Mg). For Li, Ca and Mg terrestrial weathering accounts for a considerable input, but for Rb and K there was a net accumulation in the terrestrial system. A notable difference from the other groups was also that the relative importance of the sediment as a sink was lower (except for Ba), and that there was a relatively large accumulation in the lake water and even a small export through the outlet and the talik. This indicates that the Alkali and alkaline earth metals are transported in dissolved form rather than in particulate form as the Geogenic elements and Lanthanides/Actinides. The accumulation of Ba in the sediment that cannot be explained by eolian input could be related to precipitation of barite. Thermodynamic modelling indicated that the lake water was not saturated with respect to barite at the time of sampling, but saturation was frequently observed in the pore waters so there are good reasons to suspect that barite is present in the system. It is also possible that barite occasionally is present in the eolian material.

The group *Redox sensitive elements* includes Fe, Cr, Mn and Co, and again the main source was eolian deposition and, to a lesser extent, weathering in the terrestrial system. For two of the elements (Fe and Cr), the eolian input did not fully explain the sediment accumulation, and there was also an unknown source to the lake (Rel_lakew).

The *Transition and post-transition metals* contain Zn, Cd, Sb, Bi, Sn, Cu, Mo, Ni and Pb. For most of these elements atmospheric deposition is the main source to the system, and they are retained both in the terrestrial system and in lake water. The exceptions are Ni and Pb, for which release from the terrestrial system is the most prominent source and the sediment a major sink.

The "*Halogens and boron*" comprises I, Br, Cl and B, which enter the system through atmospheric deposition. All four elements were retained in the terrestrial system, with Br, B and I showing a higher retention than Cl. The accumulation in the sediment also followed the same pattern, with I having a higher accumulation than Br, B and Cl. For Cl there was also a small export through the outlet and the talik.

"Sulphur" (S) is mainly supplied through release from the terrestrial system, and it is mainly retained in the lake water. *"Phosphorus"* (P) was supplied by eolian and atmospheric deposition, but the main source is to the system is unknown. This unknown source is also reflected in the sediment, where eolian deposition only accounts for a small fraction of the P that have accumulated in the sediments.

Field experiments

Quantification of groundwater heat advection in the active layer

This experiment aims at quantifying the role of groundwater flow and infiltration on the heat budget of the active layer for a site in continuous permafrost.

Heat transport in the ground is generally assumed to occur mainly through conductive processes in most natural environments. In the summer, this transport is directed downward from the ground surface, while in the winter heat leaves the ground and moves up to the atmosphere. This process representation forms the basis for most permafrost models today. Transport of heat with groundwater could, however, be important for the development of the active layer although the potential magnitude of these fluxes has not been well constrained across permafrost environments. In this experiment, we use observations of ground temperatures, soil moisture and ground water levels at the Two Boat Lake site to monitor the effects of groundwater on ground temperatures for natural conditions and during simulated rainfall events. Simulated rainfall experiments were conducted in August 2017 using a drip irrigation system with water of known temperature and discharge rate (Fig. 38). Statistical methods will be used to compare ground temperature gradients during different groundwater, infiltration and soil moisture conditions. A similar study for a sub-arctic saturated peatland site (Fig. 38) showed that heat advections had limited effects on ground temperatures for most of the year, but that during snowmelt heat advection resulted in rapid thaw rates in the seasonal frost (Sjöberg et al., 2016).

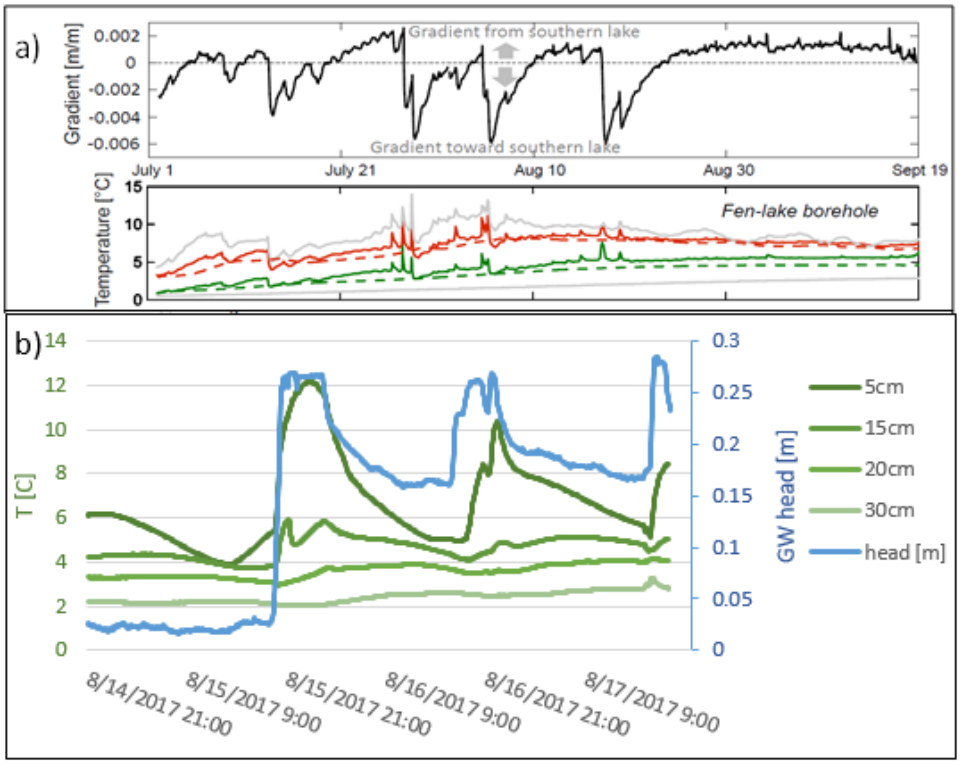

Figure 38. *Observed hydraulic gradient (a, top) and ground temperatures at different depths (a, bottom) for a fen in the sporadic permafrost zone (from Sjöberg et al., 2016). Observed groundwater table and temperatures at different depths during simulated rainfall at TBL (b).*

The GAP-project

Introduction

The first part of this section provides a general overview of the Greenland Analogue Project (GAP), including a summary of the key findings, whereas the latter part focuses on the GAP proglacial field site to be visited during this field excursion, i.e. the DH-GAP04 borehole site. Those interested in additional details are recommended a reading of the two GAP final reports; the data report, which is a comprehensive description of the data collected and field methods applied (Harper et al. 2016), and the final report, which presents the key findings from the GAP (Claesson Liljedahl et al. 2016).

GAP project overview

The GAP was a collaborative research project conducted between 2008 and 2013 by the national nuclear waste management organisations in Sweden (SKB), Finland (Posiva) and Canada (NWMO). The primary aims of the GAP were to enhance scientific understanding of glacial processes and their influence on both surface and subsurface environments relevant to the performance of deep geological repositories for spent nuclear fuel in crystalline shield rock settings. Based on its size, relative accessibility, and crystalline shield bedrock, the Greenland Ice Sheet (GrIS) was selected by the GAP as a natural analogue for glaciation processes expected to reoccur in Fennoscandia and Canada over Deep Geological Repository (DGR) safety-relevant timeframes. SKB has continued to monitor and maintain some of the GAP field installations, and is planning to carry on with the monitoring for at least another 3-4 years, but hopefully even longer.

To achieve the required increase of understanding, GAP research focused on obtaining information that contributes to answering the following six overall project questions:

1) Where is meltwater generated under an ice sheet?
2) What is the hydraulic pressure situation under an ice sheet, driving groundwater flow?
3) To what depth does glacial meltwater penetrate into the bedrock?
4) What is the chemical composition of glacial water if, and when, it reaches repository depth?
5) How much oxygenated water will reach repository depth?
6) Does discharge of deep groundwater occur in the investigated proglacial talik in the study area?

These questions cover areas where process understanding based on observations from an actual ice sheet setting or the extent of the process (in terms of duration, magnitude or scale) were very limited prior to the GAP. These questions also highlight areas where substantially conservative assumptions have been necessary in safety assessment analyses. The six project questions were deliberately formulated in a condensed and simplified fashion and they have been used only as general guidelines for planning research conducted in the GAP. In reality, each question encompasses a range of specific research goals that were included in activities conducted in the GAP.

The GAP study area (Fig. 39) is located east of Kangerlussuaq village on the west coast of Greenland and covers approximately 12,000 km2, of which approximately 70% is occupied by the GrIS. To advance understanding of glacial hydrogeological processes, GAP research activities included both extensive field work and modelling studies of the GrIS, focused into three main project areas: 1) surface-based ice sheet studies; 2) ice drilling and direct studies of basal conditions; and 3) geosphere studies. The main objectives and activities of these project areas are provided below:

1. **Surface-based ice sheet studies** aimed to improve the current understanding of ice sheet hydrology and its relationship to subglacial hydrology and groundwater dynamics. This work

was based primarily on *indirect* observations from the ice sheet surface of the basal hydrological system, to obtain information on the parts of the ice sheet which contribute water for groundwater infiltration. Project activities included quantification of ice sheet surface water production, as well as an evaluation of how water is routed from the ice surface to the interface between the ice and the underlying bedrock.

2. **Ice drilling and direct studies of basal conditions** also aimed to improve understanding of ice sheet hydrology and groundwater formation based on *direct* observations of the basal hydrological system, paired with numerical ice sheet modelling. Specific processes were investigated, including: 1) thermal conditions within and at the base of the ice sheet; 2) generation of meltwater at the ice/bedrock interface; and 3) hydrologic conditions at the base of the ice sheet. Activities included ice drilling of multiple holes at three locations on the ice sheet, at distances up to thirty kilometres from the ice sheet terminus, to assess drainage, water flow, basal conditions and water pressures at the interface between the ice and bedrock.
3. **Geosphere investigations** focused on groundwater flow dynamics and the chemical and isotopic composition of water at depths of 500 metres or greater below ground surface, including evidence on the depth of permafrost, redox conditions and the infiltration of glacial meltwater into the bedrock. Deep and inclined boreholes were drilled through the permafrost in the vicinity of the ice sheet margin. The boreholes were hydraulically tested and instrumented to allow hydrogeologic and hydrogeochemical monitoring. The nature of ground conditions under a proglacial lake was also investigated, to assess if areas of unfrozen ground within the permafrost (taliks) may act as a potential pathway for exchange of deep groundwater and surface water.

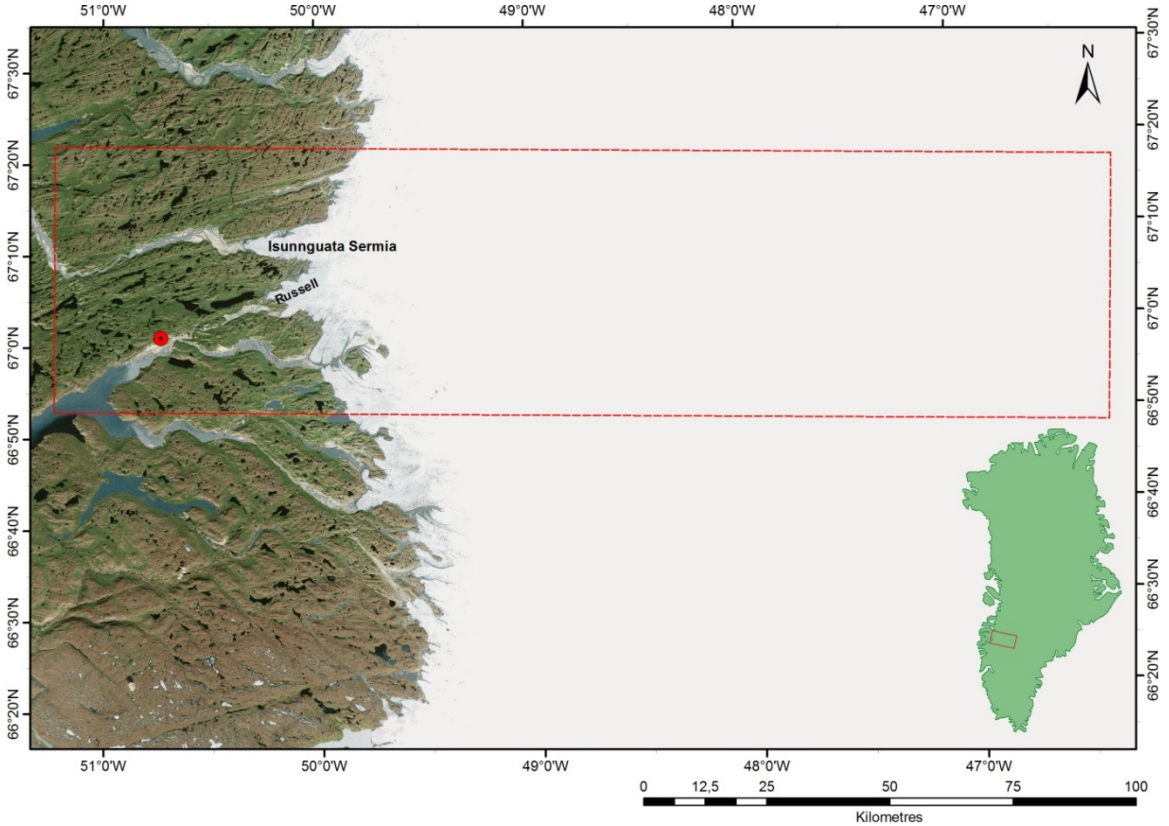

Figure 39. *Overview map showing the GAP study area (red dashed rectangle). Inset map shows the location of the study area on the Greenland scale. The key outlet glaciers in the GAP study area, Isunnguata Sermia and Russell glacier are indicated. Red circle shows the location of Kangerlussuaq village and the Kangerlussuaq International Airport (SFJ). Background image is a World Imagery esri satellite image acquired 2 October, 2014.*

The key findings from these three main project areas contribute towards improved scientific understanding of processes associated with the GrIS. Several highlights are summarised below, in terms of attributes relevant to assessing the long term safety of a DGR.

Transient meltwater processes on the ice sheet surface: Surface melt and runoff is a summer phenomenon limited to 3–4 months (May through September), during which time the ice surface lowers by up to 3–4 metres. The volume of meltwater generated at the surface each summer exceeds the amount of predicted basal melt by two orders of magnitude (cm of basal melt vs. metres of surface melt). The summer melt period therefore completely dominates the annual cycle of available water volume.

Abrupt draining of supraglacial lakes (SGLs) into newly opened fractures is one of the key mechanisms for establishing surface-to-bed pathways. Nearly all surface melt eventually penetrates the ice and reaches the bed. Just above the equilibrium line altitude (ELA), where meltwater begins to pool, is approximately the interior limit where substantial surface melt has the potential to penetrate to the bed. Seasonal variations in water flow through the basal drainage system beneath the ablation zone occur mainly as the result of ice sheet surface melting.

Basal thermal distribution and generation of water at the ice sheet bed: Direct observations made in 23 boreholes drilled to the ice sheet bed at distances between 200 m and 30 km from the ice margin provide the first direct evidence that the entire outer flank of the study area has a melted bed, with liquid water present, rather than a universally or locally frozen bed. No evidence has been found to suggest that a complex pattern of patchy frozen/melted bed conditions exist in the ice marginal areas within the region studied.

Modelling results illustrate that the location of the boundary between melted and interior frozen conditions is highly sensitive to geothermal heat flux values, but relatively insensitive to longitudinal 'pulling' caused by fast sliding ice flow near the margin. For all choices of boundary conditions and modelling parameters believed to be reasonable, a central frozen area extends many tens of kilometres from Greenland's central ice flow divide, but greater than 75% of the studied sector of the GrIS is subject to basal melting conditions.

Hydraulic boundary conditions for groundwater simulations: Hydrologic conditions at the ice sheet bed were found to vary across the width of the GAP study area. Between the ice divide and the margin, there is evidence for three different basal zones as defined by the amount and configuration of meltwater: the *frozen bed zone*, the *wet bed zone*, and the *surface-drainage bed zone*. The *surface-drainage bed zone* is further characterised by a zone with *distributed water drainage* and a zone with *transient conduit drainage* (Fig. 40). These hydrological zones result from surface, bed, and internal ice flow processes, and may be representative of Northern Hemisphere ice sheets in a similar stage of development to the current GrIS.

This revised conceptual understanding of the drainage system developed through the GAP implies that much of the bed inward of the margin is covered by water, rather than mostly drained by discrete conduits with little water in between. Further, the drainage system would not be expected to undergo large pressure drops in response to water input forcing, as hypothesised for a conduit dominated system that rapidly drains high volumes of water from the bed. Taken together, hydraulic measurements and analyses from the ice boreholes imply that ice overburden hydraulic pressure (i.e. a hydraulic head corresponding to 92% of ice thickness) provides an appropriate description of the basal hydraulic pressure as an average value for the entire ice sheet over the year.

Role of permafrost and taliks: The GAP study area is located in a region with continuous permafrost. Close to the ice sheet margin, the permafrost thickness reaches 350–400 m, as measured in the DH-GAP03 and DH-GAP04 boreholes. The main part of the base of the ice sheet in the study area, including the marginal areas, has been shown to have basal melting conditions,

with the exception of the central parts of the ice sheet. Taken together with the fact that most of the area presently glaciated was also glaciated throughout the past 10,000 years (and therefore, has not been subject to any sub-aerial permafrost development during this time), indicates that permafrost does not exist under the major part of the large, warm-based areas of the ice. An exception is at the ice margin, where a wedge of permafrost most likely stretches in under the ice. It is not known how far this subglacial permafrost wedge stretches (e.g. if it is a few hundreds of metres or several kilometres).

Where permafrost extends to depths of greater than 300 m, a lake diameter of approximately 400 m would be expected to maintain unfrozen areas through the entire permafrost thickness, e.g. through taliks, which provide a potential pathway for exchange of deep groundwater and surface water. Borehole DH-GAP01 was drilled underneath a lake ("Talik lake", by the GRASP team referred to as the Two Boat Lake), confirming for the first time, the existence of a through talik beneath a lake in an area of continuous permafrost. Furthermore, sampling of this borehole has provided the first information on groundwaters from within a talik located in close proximity to the ice sheet margin. Although it had been hypothesised that the Two Boat Lake would act entirely as a discharge feature, evidence from hydraulic head measurements and the stable water isotopic composition of the sampled groundwaters are consistent with seasonal recharging conditions occurring at this location.

Meltwater end-member water compositions: The characteristics of a meltwater end-member are needed when evaluating water compositions in glaciated areas, as well as in any numerical modelling of groundwater flow and reactive solute transport. Based on analysis of meltwater compositions conducted as part of the GAP and reported in the scientific literature, a glacial meltwater end-member has depleted $\delta^{18}O$ (–30 to –25‰) and $\delta^{2}H$ signatures (–235 to –200‰) consistent with cold climate conditions and a very low total dissolved solids content, with solute concentrations ranging from practically zero to approximately 1 mM for the main solutes, such as Ca^{2+}.

Depth of glacial recharge: The stable water isotopic signatures ($\delta^{2}H$ and $\delta^{18}O$) indicate that the groundwaters sampled in both boreholes (DH-GAP01, DH-GAP04) are of glacial meltwater origin. The millions of years of predominantly glacial conditions in this region, the local structural geology and fracture distribution, the presence of high hydraulic gradients and the presence of relatively low salinity fluids at depth in the rock mass have likely facilitated the penetration of glacial meltwaters at this site to depths of at least 500 m.

The relatively low concentrations of Na and Cl in the groundwaters likely originate from within the rock matrix through water-rock interactions and diffusion, whereas Ca and SO_4 in these waters originate from dissolution of gypsum, which occurs as a fracture infill mineral at depths below approximately 300 m. A preliminary interpretation of dissolved He concentrations suggests that the deep groundwaters may have residence times exceeding hundreds of thousands of years. Together with the extensive persistence of gypsum (hydrothermal origin) below 300 m, which is a highly soluble mineral, this suggests stable conditions with limited groundwater flow at depths below 300 m at the DH-GAP04 location.

Redox stability of the groundwater system: Below the permafrost (and/or at depths greater than about 350 m), reducing conditions are interpreted to prevail in the study area. Past penetration into the bedrock of dissolved oxygen in meltwaters has been limited in depth, as indicated by the presence of pyrite in fractures below approximately 50 m; iron oxyhydroxides are found in fractures only in the upper parts of the rock (down to 60 m), with only a few isolated occurrences of goethite down to 260 m depth.

The above examples illustrate ways in which research conducted within GAP has advanced scientific understanding of hydrological processes related to the presence of an ice sheet, including the temporal and spatial nature of processes occurring on the ice sheet surface,

conditions at the ice sheet bed (thermal and meltwater generation), and interactions between glacial meltwater and the underlying groundwater systems. In assessments of the potential risk to humans and the environment from DGRs for spent nuclear fuel, uncertainties related to process understanding are typically handled using assumptions which over- rather than underestimate the potential radiological consequences. The increased scientific understanding of glacial hydrological processes attained through the GAP, and the associated reduction of uncertainties, has provided new insights that will inform and strengthen future safety cases, including the safety assessments developed for DGRs in crystalline bedrock settings. Furthermore, the findings may allow a re-evaluation of the degree of pessimism in some of the assumptions made in previous safety assessments and modelling work.

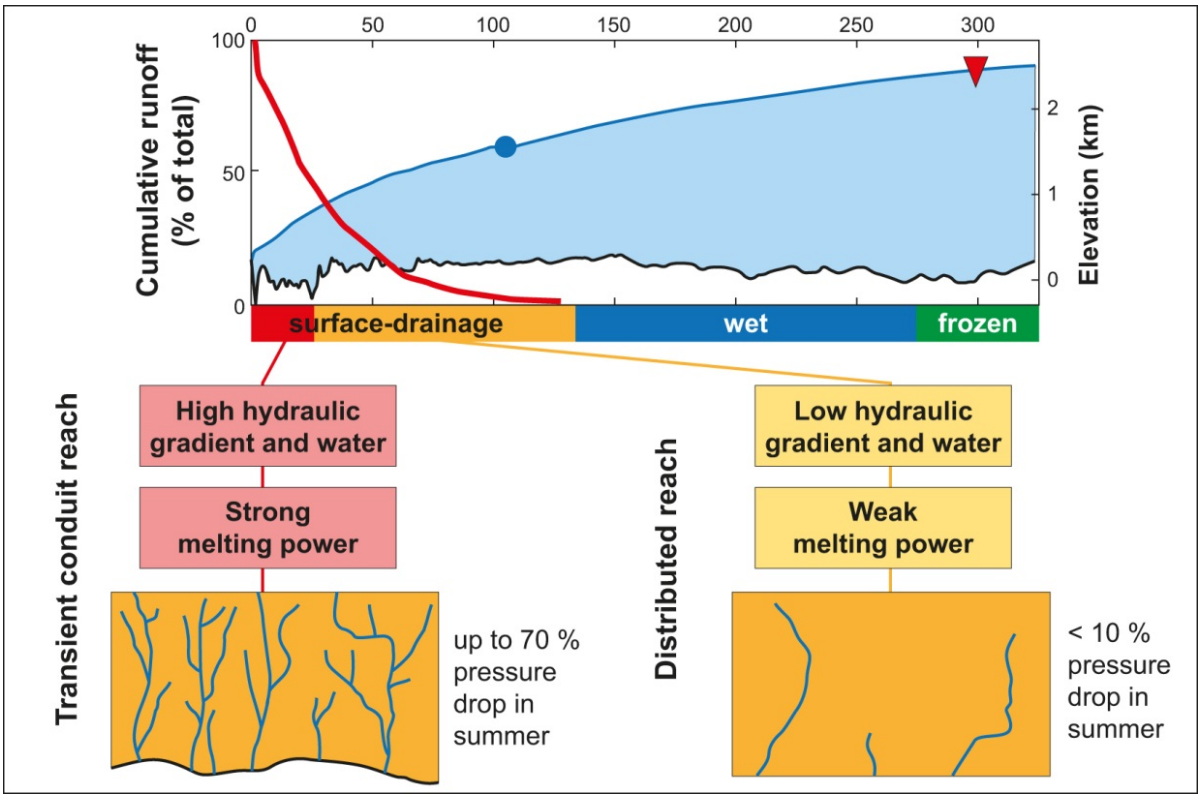

Figure 40. *Schematic cross section through GAP study domain from the ice divide to the terminus of Isunnguata Sermia. Top panel shows ice surface and bed; blue dot on surface is the equilibrium line (ELA), and red triangle is the 20 year average extent of any surface melt. Red line shows 1958–2013 average meltwater runoff, accumulated from high-to-low along the ice surface, from the MAR model (Tedesco et al. CCNY Digital Archive). The top panel also shows the location and size of the three identified basal hydrological zones (here coloured red/yellow, blue and green below the ice sheet), see the text. Bottom of panel shows a conceptual view of subglacial conditions.*

Figure 41 is a synthesis figure of the main results and key hydrogeological and hydrogeochemical findings from the GAP (Claesson Liljedahl et al. 2016).

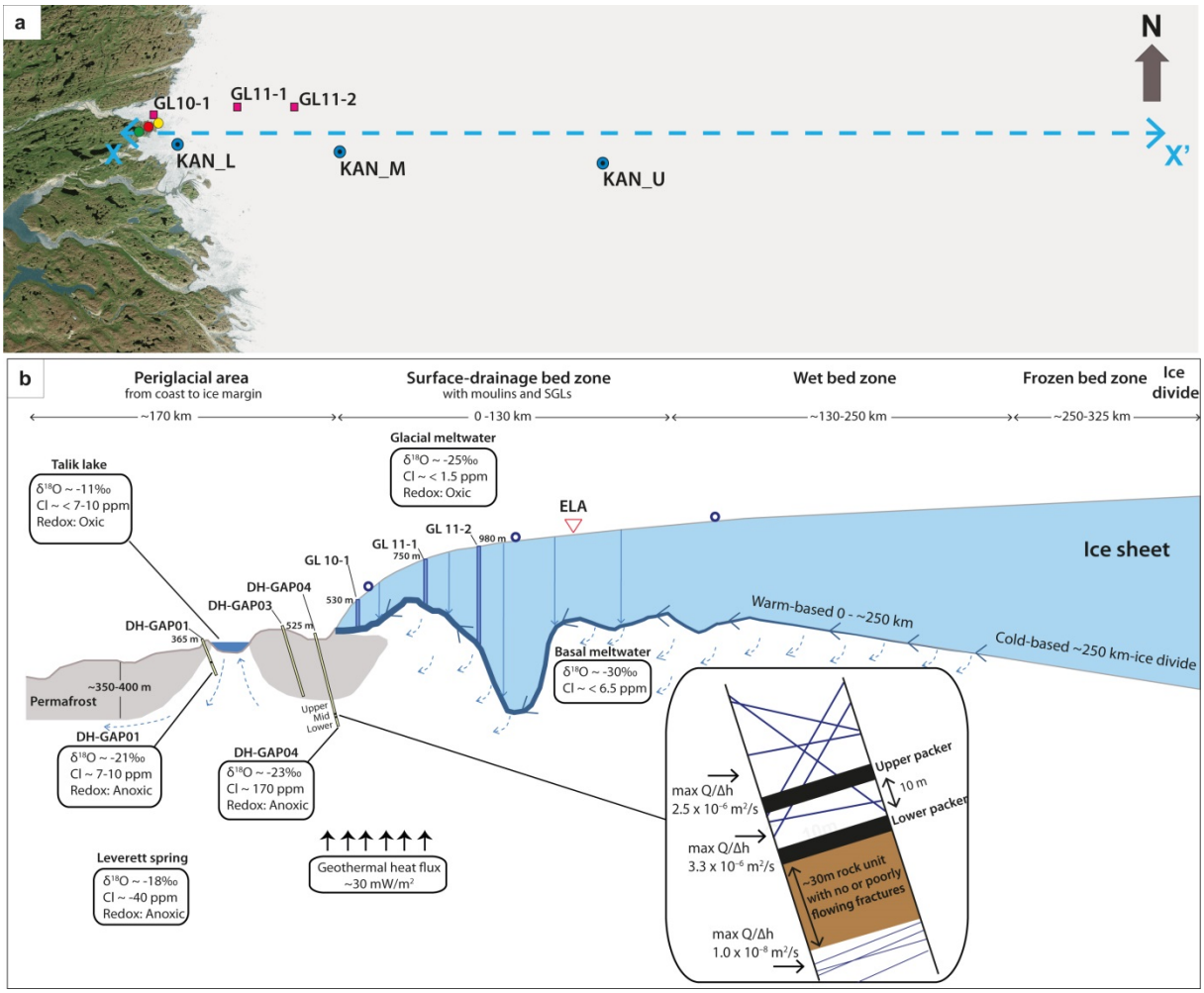

Figure 41. *Synthesis of main results and conceptual understanding of the hydrology within the GAP study area. a) View showing extent of the area where GAP field investigations and ice sheet modelling were carried out. Automatic weather stations (AWS) shown as blue circles. Locations of ice boreholes GL 10-1, GL 11-1 and GL 11-2 shown as pink squares. Bedrock boreholes shown as coloured circles, where green = DH-GAP01, red = DH-GAP03 and yellow = DH-GAP04, respectively. The dashed blue line (X to X') denotes the approximate extent of the cross-section seen in the lower panel. b) Schematic cross-section highlighting key GAP data and conceptual hydrological and hydrogeochemical understanding. Ice boreholes shown as blue lines are projected from a few km out of plane of the transect. The different glaciohydrological basal zones in the upper part are from Figure 39. Note that the position of the frozen-melted boundary (FMB) zone is based on modelling results. Blue line at the ice sheet bed indicates basal flow. Numerical figures beside bedrock and ice boreholes represent measured hydraulic heads. Main hydrogeochemical results from GAP key locations are shown in boxes. No redox data could be collected from the basal meltwaters. Note the presence of permafrost near the ice sheet margin, including the existence of a through talik under the Talik lake (In this guide also referred to as TBL). Recharge into the through talik was documented by the GAP data. Although not observed in this study, groundwater discharge could potentially also occur in the same talik, as indicated in the figure. Also note the considerable subglacial bedrock relief. Red triangle shows the approximate location of the ELA. Inset in b shows a schematic view of the fracturing and the measured transmissivity values around the monitoring sections in DH-GAP04 (see inset c in Fig. 45).*

GAP field visit location – the deep research borehole site (DH-GAP04)

The aim of the GAP geosphere investigations was to increase the understanding of hydrogeochemical and hydrogeological conditions in the bedrock down to repository depths (500 to 1,000 m). These studies were planned and designed to directly or indirectly address the following questions: *To what depth does glacial meltwater penetrate into the bedrock, What is the chemical composition of glacial water when and if it reaches repository depth?, How much oxygenated water will reach repository depth?,* and *Does discharge of deep groundwater occur in the investigated proglacial talik in the study area?* In addition to the questions listed above, the geosphere investigations provided indirect information to address the question *What is the hydraulic pressure situation under an ice sheet, driving groundwater flow?*

The main geosphere activity in the GAP was the drilling and instrumentation of three cored bedrock boreholes, DH-GAP01, DH-GAP03 and DH-GAP04 (Fig. 42, 43 and Table 4). These boreholes were drilled in order to: 1) study a potential through talik beneath a lake (DH-GAP01); 2) define the depth of permafrost close to the ice margin (DH-GAP03); 3) collect drill core material for geological and structural studies (DH-GAP01, DH-GAP03 and DH-GAP04); and 4) provide groundwater sampling, hydraulic testing opportunities and to allow groundwater monitoring (DH-GAP01 and DH-GAP04).

Bedrock geology

In order to enhance understanding of the geology and structure of the study area, geological mapping of the region was conducted during 2008–2013. Detailed geological investigations included scanline mapping of fractures and faults and characterisation of the foliation and main rock types at seven different key locations in 2008 (Aaltonen et al. 2010). Later mapping campaigns aimed at increasing the general understanding of the complex geology of the area and providing sufficient information to generate a geological map of the drilling sites (SKB 2010b, Harper et al. 2011, Harper et al. 2016). Detailed geological mapping focused on a transect extending from Kangerlussuaq to the ice margin and a smaller subarea surrounding the sites selected for the drilling of the three boreholes. Aeromagnetic lineament interpretation and ground-truthing of these lineaments was also done within the site area. Due to several generations of large-scale folding overprinting the bedrock, the site area (in close proximity to the three boreholes) shows a complex geology (e.g. Engström and Klint 2014). Drill core investigations included detailed fracture characterisation, lithological mapping, and mapping of foliations and deformation zones (Pere 2014).

The rock types in the boreholes can be divided into four main types: felsic gneiss, mafic gneiss, intermediate gneiss and granitic pegmatite. The relative amount of mafic/felsic minerals have been used as a guideline when defining the rock types. The felsic gneisses consist typically of K-feldspar, quartz and plagioclase with some biotite. The mafic gneisses typically are massive or slightly foliated and contain large amounts of garnet with amphibole and pyroxene. The intermediate gneisses resemble mafic gneisses but contain more plagioclase and biotite than amphibole and pyroxene. DH-GAP01 is situated in foliated felsic gneiss which has both mafic and intermediate layers. In DH-GAP03, alternating layers of felsic and mafic gneisses dominate. DH-GAP04 is dominated by mafic garnet gneiss in the upper 300 m, with more foliated intermediate to felsic gneiss below. For a comprehensive presentation of the core logging, see Pere (2014).

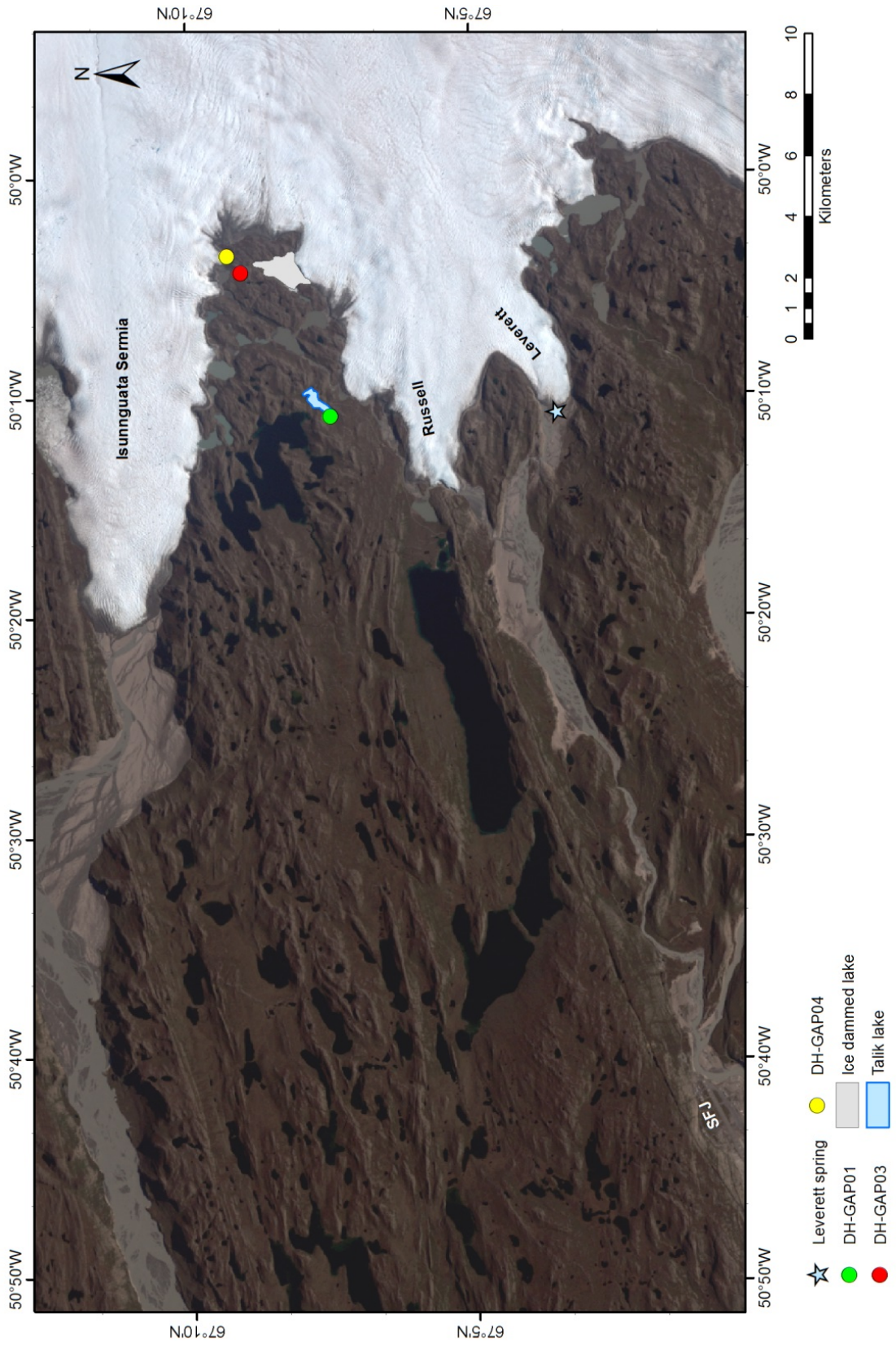

Figure 42. *Map of the area where geosphere investigations were carried out. The key geosphere investigation and monitoring sites: bedrock boreholes, the Leverett spring, Talik lake and the Ice dammed lake, are highlighted. SFJ = Kangerlussuaq International Airport. Background Landsat image was acquired 23 August, 2000.*

Table 4. Technical details of boreholes DH-GAP01, DH-GAP03 and DH-GAP04. Elevations are in m relative to the WGS-84 ellipsoid. TOC = top of casing, EOH = end of hole.

Borehole	Top of Casing (TOC) elevation (m)	Borehole length (m)	Vertical depth below TOC (m)	Elevation of end of borehole (EOH) (m)
DH-GAP01	374.7	221.5	190.7	184.0
DH-GAP03	484.9	341.2	321.7	163.2
DH-GAP04	526.2	687.0	649.1	–122.9

Figure 43. *Photo showing the drilling of borehole DH-GAP04. Photo taken by Anne Kontula.*

Bedrock drilling

Two 57 mm (DH-GAP01 and DH-GAP03) and one 76 mm bedrock (DH-GAP04) boreholes were drilled by the GAP using standard core drilling techniques (Fig. 42 and Table 4). DH-GAP01 is the shallowest and DH-GAP04 the deepest; hydrogeological data were successfully acquired from these two boreholes. Due to technical problems, only temperature information was obtained from DH-GAP03. DH-GAP04 is drilled approximately 200 m from the ice margin of the Isunnguata Sermia outlet glacier. DH-GAP03 is located approximately 800 m SW of DH-GAP04. Both boreholes are interpreted to penetrate a tight synformal syncline that dips gently under the Isunnguata Sermia margin. DH-GAP01 is located approximately 6 km SW of DH-GAP04 and approximately 1 km from the nearest ice margin (Fig. 42).

Due to the presence of permafrost and the risk of freezing limiting the time available for borehole testing and instrumentation, the drilling was performed with heated (up to 60°C) drilling water. A local, geochemically well-characterised water source was used as drilling water

(Harper et al. 2016) and the drilling water was further spiked with sodium fluorescein dye ($C_2OH_{10}Na_2O_5$) to evaluate the drilling water contamination in subsequent geochemical sampling.

Borehole DH-GAP04

The aim of this borehole was to provide groundwater sampling and monitoring opportunities down to, or below, typical nuclear waste repository depths (approximately 500 m or more), and it was intended that the hole would extend beneath the ice sheet (Harper et al. 2011). The borehole was drilled towards the north with an inclination of 70° from horizontal at approximately 210 m from the ice margin (Fig. 44). The bottom of the hole is under the ice sheet, approximately 20 m beyond the ice margin. However, it should be recalled that the GrIS is currently melting and thinning, and although the melt is not as substantial in the GAP study area as within other parts of the ice sheet, the ice margin has retreated a few metres at the borehole site during the course of the project. The upper 2.5 m of the borehole are cased. DH-GAP04 is fairly evenly fractured, but contains intact sections. The average fracture frequency is 1.97/m (Pere 2014, Harper et al. 2016). The same pond that was used for drilling water for DH-GAP03 was also used when drilling this hole.

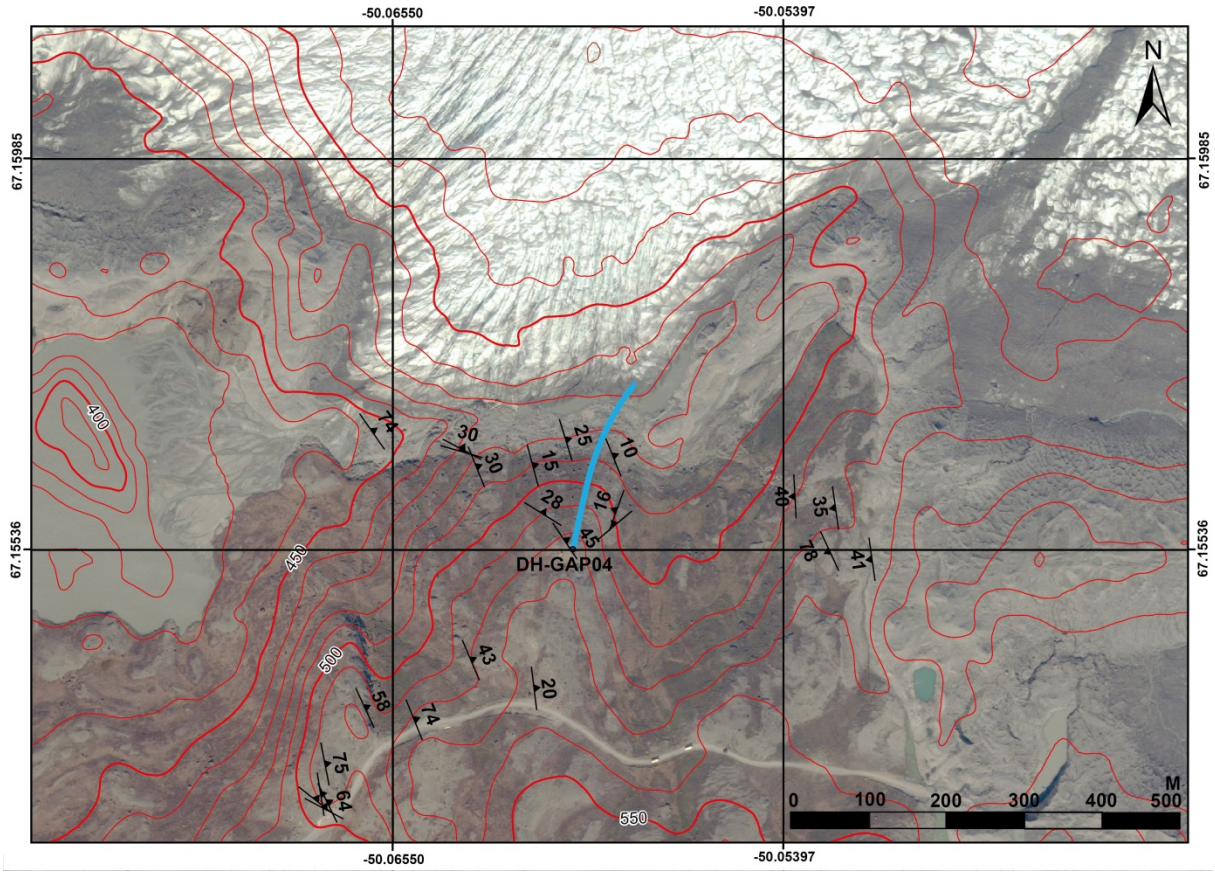

Figure 44. *Location of the DH-GAP04 drilling site with the trace of the borehole (blue line). Foliation measurements are given, indicating the strike, dip direction and dip angle. Red lines are elevation contours with a 10 m interval. Background image is a Quickbird acquired 4 July, 2011, which is when DH-GAP04 was drilled.*

Hydraulic testing using the Posiva Flow Log (PFL) method was done after completion of drilling to identify flowing fractures to optimise the positioning of the downhole instrumentation. The primary motivation for carrying out PFL testing in DH-GAP04 was to find the best location for the downhole instrument system; however, the data from the PFL testing were useful also for hydrogeological characterisation of the tested bedrock volume, a requirement to understand the hydrogeology of the ice marginal area. The PFL testing identified nine flowing features (Fig. 45). The measured specific capacities (flow rate in m^3/s per metre of head change) in these flowing features range from $1.6 \cdot 10^{-9}$ to $3.3 \cdot 10^{-6}$ m^3/s.

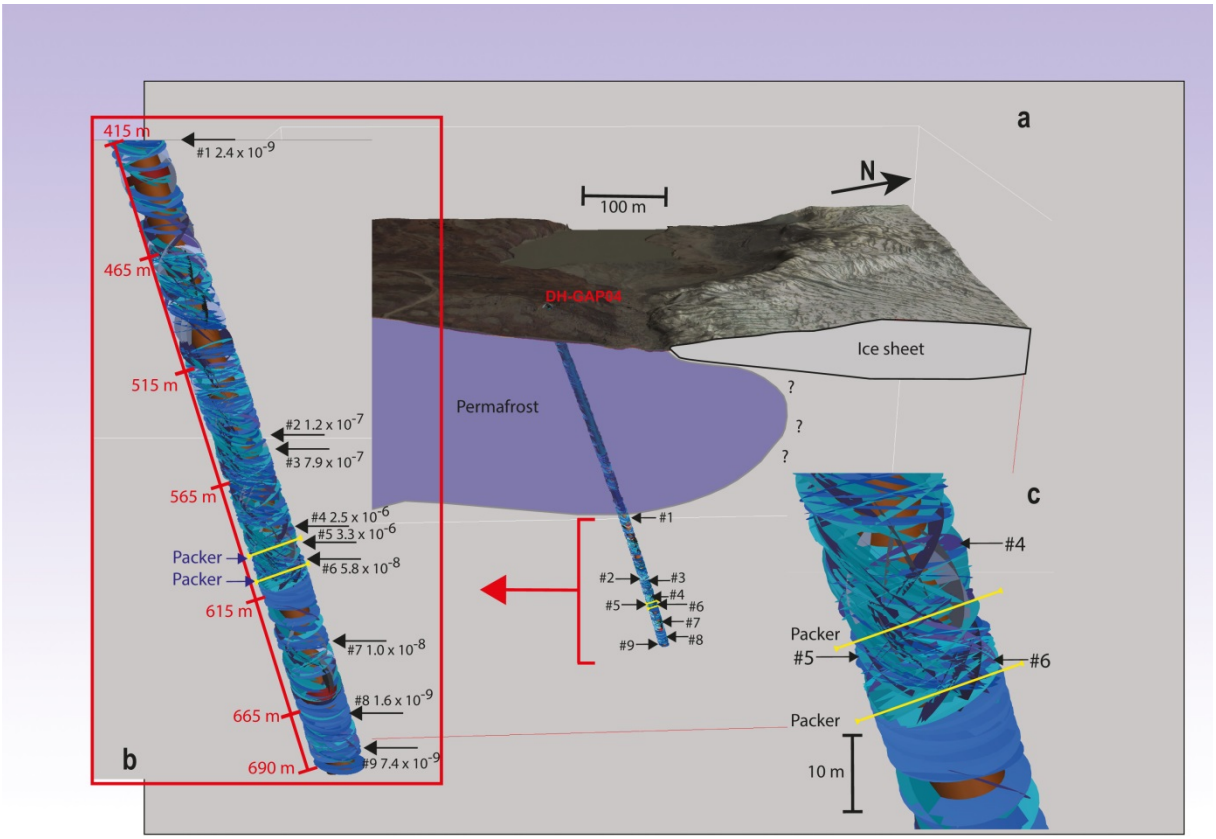

Figure 45. *Visualisation of all fractures mapped in the unfrozen part of DH-GAP04 and water-conducting features (indicated by arrows). Purple area denotes permafrost. Inset on the left (b) shows the fracture characteristics below the permafrost. Measured specific capacities (flow rates in m3/s per metre of drawdown) are shown for the nine water conducting features in figure (a). Inset on the right (c) gives a detailed view of the fracturing around the packed-off section (Sect-mid). An approximately 30 m thick unit of significantly less fractured bedrock (between 604–638 m borehole length) exists just below the packed-off section. The few fractures in this unit have almost uniformly sub-horizontal orientations.*

Following the PFL survey, the borehole was instrumented to provide information about the hydrogeochemical and hydrogeological conditions. The instrumentation contains a two-packer system (each packer is 1 m long) isolating a section between 561 to 571 m vertical depth (i.e. from top of upper packer to top of lower packer), dividing the hole into three sections (Fig. 46). The upper 400 m of the borehole are frozen since this part is within permafrost. The sections are named: the upper section (Sect-up), the mid-section (Sect-mid) and the lower section (Sect-low) and are all equipped with both pressure and electrical conductivity sensors. The mid-section is also equipped with a temperature sensor. A fibre optical cable extends from the surface down to the lowermost packer and allows temperature profiling.

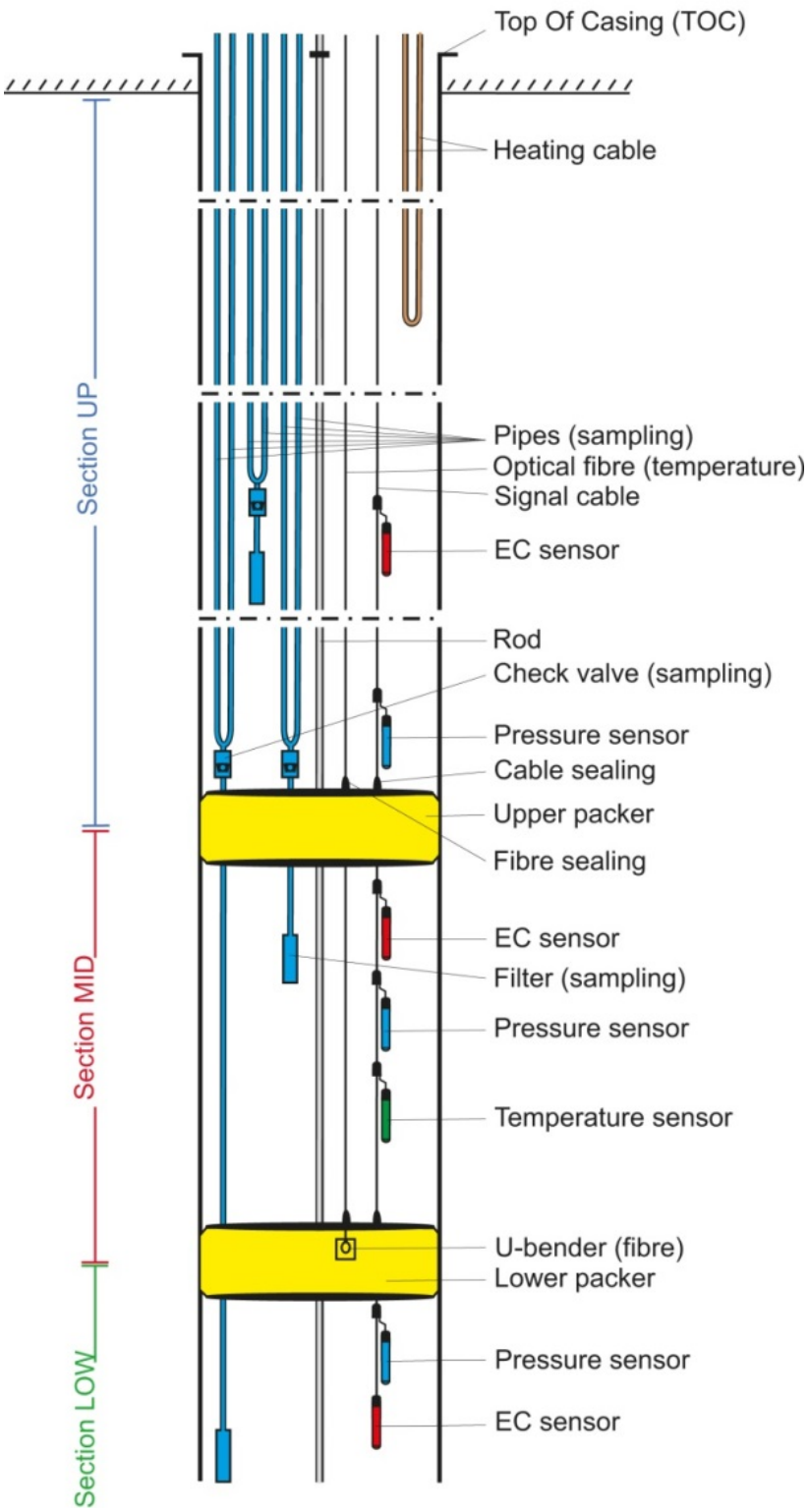

***Figure 46**. Equipment in borehole DH-GAP04. Each packer is 1 m long. The upper 400 m of the hole is within the permafrost and is naturally sealed with ice within this part of the hole. The top of the upper packer is located at a depth of 561 m below TOC. The top of the lower packer is located at a depth of 571 m below TOC. Sect-up is approximately 190 m and extends from the base of the permafrost to the uppermost packer, its volume is 840 L. Sect-mid is isolated by the two packers and is 10 m long and has a volume of 44 L. Sect-low is 80 m long and extends from the lowermost packer to the bottom of the hole with a volume of 350 L. A heating cable is installed to a depth of approximately 450 m allowing melting of the water within sample tubes for water sampling campaigns.*

Key hydrogeological findings from DH-GAP04

Through the drilling, instrumentation and sampling of borehole DH-GAP04, a first-of-its-kind inclined cored borehole beneath the margin of a continental ice sheet, the GAP obtained information on bedrock hydrogeology at vertical depths down to approximately 650 m.

The most striking result obtained from the hydrologic monitoring in DH-GAP04 is the prompt responses of the confined (artesian) hydraulic heads in the two upper sections in DH-GAP04, and how the recorded pressure changes in these two sections harmonise with the timing of the calculated seasonal ice sheet meltwater runoff (Fig. 47 and 48). The repeated observation and reporting of the multi-year consistency in timing between the recorded hydraulic head transients in DH-GAP04 at approximately 520 m vertical depth below the ice sheet margin and the seasonal changes in the superficial meltwater runoff is another unique contribution of the GAP. It is hypothesised that the pressure changes at depth are linked to the seasonal development of the basal drainage system. Specifically, the hydraulic head falls in Sect-up and Sect-mid when an efficient drainage system develops under the ice sheet during the melting season, whereas the hydraulic head builds up during winter conditions when no surface water enters the basal drainage system which then closes.

The observation of pressure responses at great depth due to hydrological perturbations at the surface has been recorded for temperate climate conditions at the Forsmark site during rain events (Follin et al. 2007); however, the unique contribution within GAP is the finding that ice sheet surface melting may result in fast pressure changes at depth in the bedrock. It is noted that these pressure changes are observed in the two upper-most sections while the lower section reacts less; this further indicates that these deeper parts of the bedrock may be more isolated from the surface.

It is concluded that the assumption of a hydraulic head in the basal drainage system equal to 92% of the ice thickness is not necessarily conservative in the sense of being overly pessimistic. Rather it appears to be the typical state based on data, from the ice holes drilled through the Isunnguata Sermia Glacier, except for the most near-frontal parts of the ice sheet. Therefore, using the ice sheet overburden pressure as a pressure boundary condition in groundwater modelling appears to be a reasonable and realistic assumption.

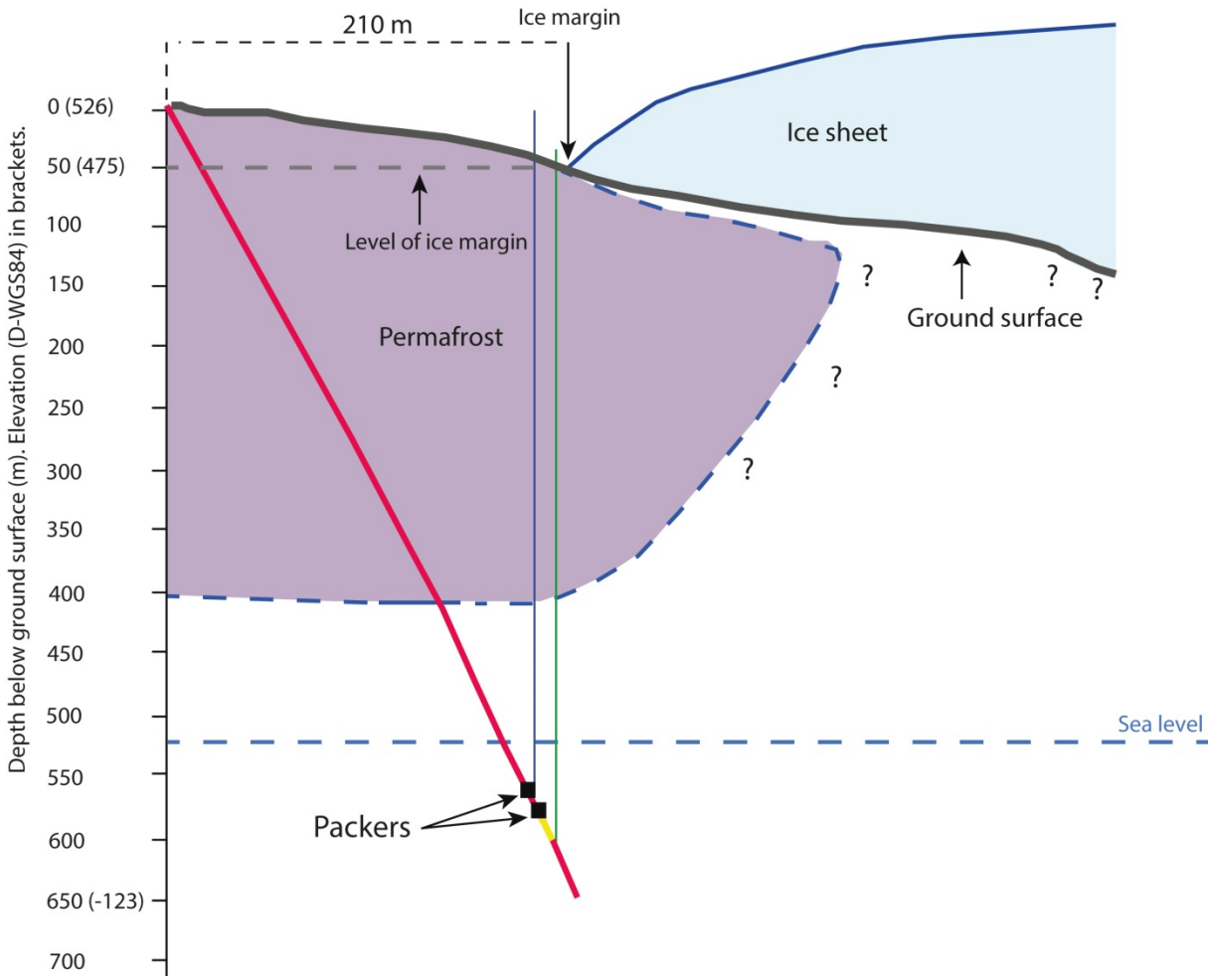

Figure 47. *Schematic illustration of the ice sheet (light blue), permafrost (purple) extent and borehole DH-GAP04. The water levels in all three borehole sections are artesian with respect to the ground surface where the borehole extends in under the ice sheet (+475 m above the WGS-84 reference ellipsoid). The vertical green and blue lines represent the head values in Sect-low (+485 m) and Sect-mid (+520 m), respectively. The head in Sect-up is identical to the head in Sect-mid. The yellow colour shading along the borehole below the lower packer illustrates the approximately 30 m intact rock unit found at this depth in the borehole.*

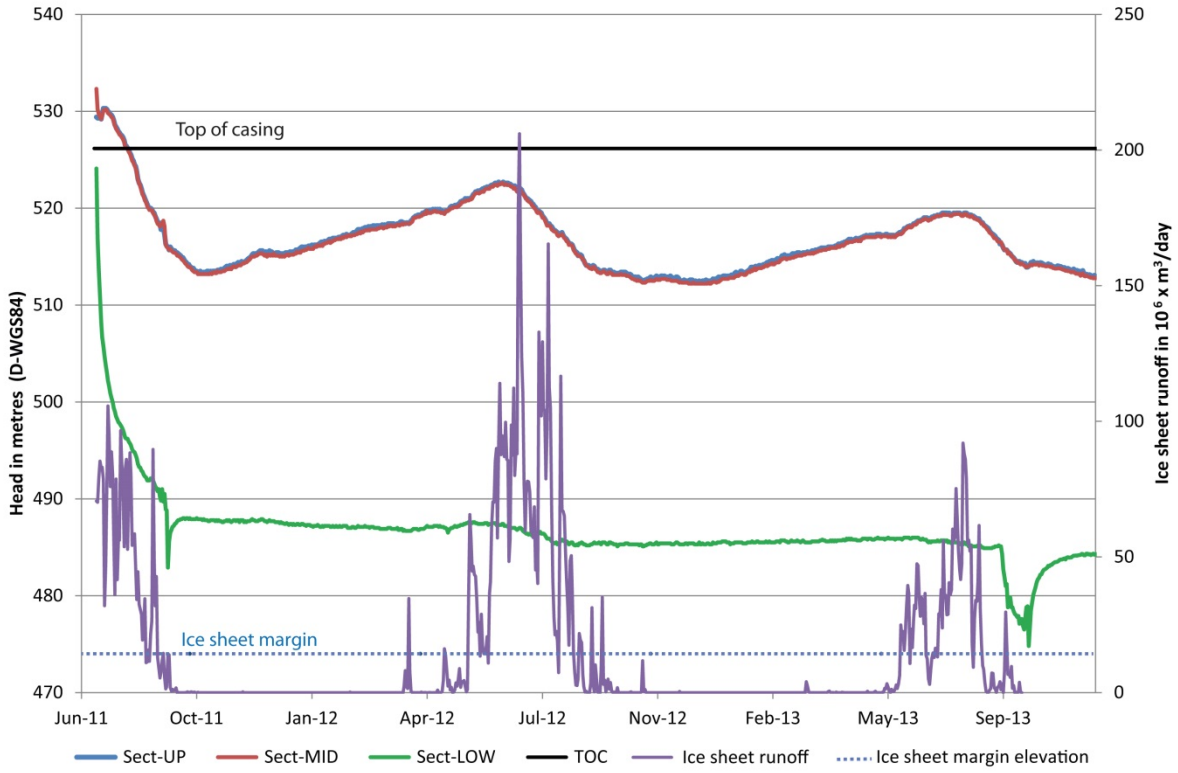

Figure 48. *Daily average hydraulic heads in Sect-up, Sect-mid and Sect-low in borehole DH-GAP04 and surface meltwater runoff from the Kangerlussuaq sector of the GrIS. Runoff in the figure is represented as total modelled runoff within the delineated ice sheet surface catchment. Note that the head curves for Sect-up (blue curve) and Sect-mid (red curve) overlie each other. TOC stands for top of casing. The dashed line shows the elevation of the ice sheet margin, indicating that pressure levels in the borehole are artesian. Successful water sampling campaigns were carried out in all sections in September 2011 and 2013.*

Key hydrogeochemical findings from DH-GAP04

Where permafrost occurs, depending on its depth, groundwaters within the shallow bedrock may be completely frozen. At the ice sheet margin, permafrost was observed to extend from the surface to approximately 350 m vertical depth. Hydraulic testing was not conducted in the upper 350 m of bedrock due to the presence of permafrost. In the temperature profiles for DH-GAP04, no evidence for water-conducting features was observed between the ground surface and the bottom of the permafrost, despite the presence of open fractures as observed in the drill core. This demonstrates effective sealing of any potentially transmissive fractures by permafrost. Groundwaters of Ca-Na-SO^4-Cl type were collected from deeper within the bedrock (more than 300 m), from three monitoring sections located between 400 and 650 m (vertical depth) in DH-GAP04. The salinity of the groundwater in the lowest monitoring section was approximately 170 mg/L Cl. The salinity of groundwaters in the upper and middle sections are likely similar, once corrected for the approximately 35% drill fluid remaining in the samples.

Corrected stable water isotopic signatures (corrected for remaining drill fluid contamination) for waters from the upper and middle monitoring sections are similar: $\delta^{18}O$ – 25 ± 0.5‰, $\delta^{2}H$ – 190 ± 3.6‰ and $\delta^{18}O$ – 24 ± 0.4‰, $\delta^{2}H$ – 180 ± 3.3‰, respectively. Groundwater from the lower section (Sect-low) also has a similar isotopic composition ($\delta^{18}O$ – 23.9 ± 0.3‰, $\delta^{2}H$ – 178 ± 2‰). All three groundwaters are at the enriched end of the range of stable water isotopic signatures measured for meltwaters ($\delta^{18}O$ – 23 to –35‰), indicating recharge during cold climate conditions (Fig. 49). The presence of dissolved Fe(II) and Mn in the groundwaters suggests conditions are anoxic and gases sampled in the upper interval contain CH_4 and H_2, which is also consistent with reducing conditions in the groundwater. In the lowest section of the borehole, ^{3}H is below detection (less than 0.8 TU) in the groundwater. A preliminary interpretation of dissolved He concentrations from the upper section of DH-GAP04 suggests that the deep groundwaters may have residence times exceeding hundreds of thousands of years.

A distinctive aspect of the geology in DH-GAP04 is the presence of abundant gypsum in fractures below 300 m vertical depth. Gypsum present as fracture infillings has a cross-fibrous mineralogical texture suggesting a high temperature (hydrothermal/metamorphic) origin. Gypsum was also identified as very fine to fine-grained, rounded crystals dispersed in the rock matrix in core samples from depths between 501 and 652 m borehole length (Eichinger and Waber 2013), or approximately 470 to 612 m vertical depth.

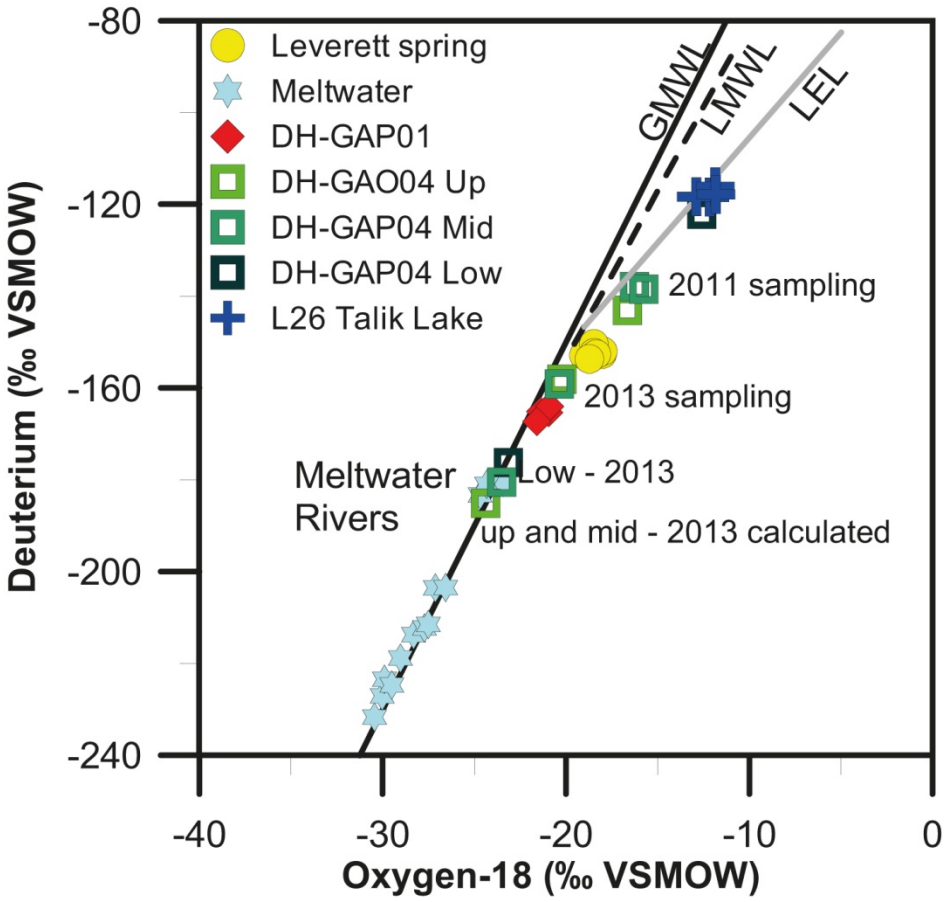

Figure 49. *$\delta^{18}O$ versus $\delta^{2}H$ for groundwaters, meltwaters and the Two Boat Lake (L26, the lake overlying DH-GAP01). The calculated isotopic composition of DH-GAP04 waters is based on a simple linear mixing model. LEL is the local evaporation line, and LMWL is the local meteoric water line.*

Above 300 m in DH-GAP04, only a few, single gypsum-filled fractures occur. Below 300 m, the increased abundance of gypsum-filled fractures coincides with a change in rock type from mafic to felsic/intermediate gneisses, suggesting that the distribution of gypsum currently observed in the fractures may be related to the rock type available for interaction with hydrothermal fluids when precipitation of the fracture minerals occurred.

There is currently no groundwater flow in bedrock above 400 m depth in the vicinity of DH-GAP04 as a result of freezing conditions within the permafrost. However, under warmer climate conditions in the past, recharge through the fractures in this upper section could have dissolved gypsum, if originally present. This interpretation is consistent with evidence for past recharge of oxygenated waters to a maximum depth of 260 m, as indicated by the presence of iron oxyhydroxides in fractures. Although pyrite is observed in fractures below 300 m, iron hydroxide minerals were not observed. Taken together with the extensive persistence of gypsum below 300 m, which is a highly soluble mineral, there is strong evidence of stable conditions with limited groundwater flow since precipitation of gypsum at depths below 300 m. Low groundwater flow in the bedrock surrounding the monitored sections in DH-GAP04 is supported both by hydrogeological observations and hydrogeochemical observations (in particular, dissolved He concentrations.

These observed differences in past groundwater flow between the shallow and deeper systems likely reflect, in part, the existence of vertical fractures in the upper 300 m of bedrock as observed in DH-GAP04, whereas below 300 m, vertical fractures become rare and sub-horizontal fractures dominate.

Groundwater evolution

Groundwaters from within the shallow and deep bedrock evolved from meltwater recharge (Na-K-HCO_3 type, Graly et al. 2014) followed by water-rock interactions. Interaction of these meltwaters with higher salinity porewaters within the matrix, as identified in out-diffusion and crush and leach studies resulted in increased concentrations of sodium and chloride in the groundwaters. Dissolution of gypsum is an important process as groundwater travels along fractures, strongly influencing the chemical composition of groundwaters; in particular, those sampled from DH-GAP04. This interpretation is supported by the similarity between the sulphur and strontium isotopic signatures ($\delta^{34}S$, $^{87}Sr/^{86}Sr$) of the groundwaters and those of the fracture minerals, gypsum and celestite.

Tobias Lindborg
Swedish Nuclear Fuel and Waste Management Co
Box 3091, SE-169 03 Solna
Phone +46 8 459 84 00
skb.se